1-1-1982

Creep of tee branch pipe connection under internal pressure.

Takenori Shindo

CREEP OF TEE BRANCH PIPE CONNECTION UNDER INTERNAL PRESSURE

by

Takenori Shindo

A Thesis

Presented to the Graduate Committee

of Lehigh University

in Candidacy for the degree of

Master of Science

in

Mechanical Engineering

Lehigh University

1982

CERTIFICATE OF APPROVAL

This thesis is accepted and approved in partial fulfillment of the requirements for the degree of Master of Science.

July 29, 1982
(date)

Professor in Charge

Chairman of the Department

ACKNOWLEDGEMENTS

The author wishes to express his sincere thanks to his advisor, Professor D.P. Updike, for his guidance, his kind direction and encouragement. The author also wishes to express his gratitude to Professor A. Kalnins for his helpful consultation, his kind advice on the computer work.

The author would like to express his appreciation to Mr. I. Fukuda, who is the president of Babcock-Hitachi K.K., his financial support for my study and living in the United States of America.

The author would like to give thanks to his dear parents, and his dearest wife for their endless encouragement and blessing.

The author would like to express his appreciation to Mrs. Donna Reiss for her help in typing the manuscript.

TABLE OF CONTENTS

LIST OF FIGURES

LIST OF TABLES

NOMENCLATURE

E	Young's modulus of elasticity
ν	elastic Poisson's ratio
U_o	material creep rate parameter
S_o	material creep strength
n	creep exponent, $n \geq 1$
σ_e	equivalent stress
Q	transverse shear force per unit circumference
u	axial displacement in cylindrical shell
β	rotation of shell normal
w	radial displacement of cylindrical shell
σ_x, σ_θ	stress component
ε_x, ε_θ	strain component
N_x, N_θ	components of membrane stress resultant
M_x, M_θ	components of bending moment per unit length
R	main pipe radius
r	branch pipe radius
s	arc length of shell meridian and nominal stress in branch, pr/t
S	nominal stress in main, pR/T
T	main pipe thickness
t	branch pipe thickness and time
τ	time or pseudo time
p	internal pressure

x coordinate along meridian in branch

X coordinate along meridian in main

Dots over variables indicate rates with respect to time

Subscript x refers to direction along meridian

Subscript θ refers to circumferential direction

Subscript z refers to thickness direction

Subscript m refers to main pipe

Subscript b refers to branch pipe

Bars over quantities indicate their values at the edge $X=0$, $x=0$.

ABSTRACT

The creep behavior in the crotch region of two normally intersecting cylindrical pipes of different diameter and thickness is treated with the aid of an axisymmetric shell model. This model has a transfer matrix which enforces required equilibrium and continuity conditions between a branch and a main pipe. The results by the model are checked, and it is confirmed that the presented model here can analyze any combination of diameter and thickness of a tee branch connection under internal pressure in both elastic and creep analysis provided the shells are thin and the branch pipe diameter is greater than one third the main pipe diameter.

Three typical kinds of tee branch connections, which have radius ratio of 0.5 in branch and main, are analyzed using the model. The three kinds of tees are: (1) the case of equal strength in the branch and the pipe, (2) the case of equal thickness in both pipes and (3) the equal strength tee with reinforcement on the main pipe.

First of all, the case of equal strength is studied in detail including the calculation of stress redistribution and stationary creep strain rate. For the other cases, the results are discussed in contrast to the case of equal strength. The effects of reinforcement are discussed, and a recommendation for

a design of a tee branch connection is presented. Also, it is shown that elastically calculated strain rates are much larger than stationary creep strain rates and that the former will predict a creep rupture time very much shorter than the later.

1. INTRODUCTION

Structures subjected to steady tensile loading over long periods of time while they are exposed to a high temperature environment fail by either the accumulation of excessive creep deformation or by creep rupture. Such damage is one of the dominant failure modes in structures which must operate at high temperatures for long periods of times, e.g., advanced nuclear reactors, chemical plant pipe lines, coal gasification vessels and solar energy "power towers." Therefore, as such structures operate at increasingly higher temperatures, designers then must consider what amount of creep damage can be tolerated during the required service life.

Due to stress concentration, the time to failure of a thin-walled pressure vessel with unreinforced cutouts, nozzles, and shell intersections may be much less than that of a pressure vessel of the same thickness without openings subjected to the same loading and environment. Therefore, life predictions on the basis of the nominal membrane stresses of the vessel might lead to an unsafe design. As creep develops, the stresses in the regions of stress concentration redistribute and decrease.

Furthermore, life predictions based on stresses calculated by elastic analysis may result in an overly conservative design because such elastic analysis can not account for the redistribution of stress with increasing creep strain. If the loading

remains constant, the stress distribution asymptotically approaches a stationary state as the creep strains become dominant over the elastic strains. This transient takes place rather quickly and is essentially completed while the maximum creep strains are still of elastic order. Therefore, under steady loading, most of the creep life of the structure will take place while the stress state is that of the stationary state.

For the tee branch pipe connection such as shown in Fig. 1, the life prediction accounting for the stress redistribution is very costly and time consuming problem if solved by the three-dimensional finite element method.

D.P. Updike and A. Kalnins showed a very simple and accurate method to solve a complex creep problem of intersecting equal diameter cylindrical shells under internal pressure [1].

Using the presented equation in [1], a designer can predict a life of such three-dimensional intersecting structure easily and at less cost than would be required by three-dimensional finite element methods.

Here we extend the method shown in [1] to the problem of the structure consisting of intersecting pipes of unequal diameter and thickness pipe under creep behavior. To make the required equilibrium and continuity condition between two different diameter intersecting pipes, a special transfer matrix is needed in the model.

The validity of the transfer matrix is checked and the results are compared with published solution from some references.

Finally, the analysis is applied to three typical kinds of tee branch connections of which all radius ratios are 0.5 in the branches and mains. These are: (1) the case of equal strength branch and main, (2) the case of equal thickness in branch and main and (3) the case of reinforced equal strength tee.

The results are carefully studied and examined including stress distributions and stationary creep strain rate. The magnitude of stress redistribution and the effect of a reinforcement are also discussed.

II. METHOD OF ANALYSIS

In reference [2] the calculation of the peak elastic stresses of a tee branch pipe connection under internal pressure are shown. This analogy is as follows.

Referring to Fig. 2, the tensile forces on the cross section $C_bB_bAB_mC_mJK$ of the structure are set equal to the resultant force of the pressure acting on area $C_bB_bAB_mC_mJK$. If it is assumed that both the main pipe and the branch are long and that the stress along KJ is the nominal hoop stress, then the pressure times area EC_mJK is balanced by the tensile force along C_mJK. This then requires that the tensile force on $C_bB_bAB_mC_m$ balance the pressure times area $C_mB_mAB_bC_bE$. The force balance equation then becomes

$$\int_{C_bB_bAB_mC_m} N_\theta dx - pRL_m - prL_b = pRr \qquad (1)$$

Expressions for the edge shearing forces Q_{xm} and Q_{xb} acting on the cylindrical panels $AB_mM_mL_m$ and $AB_bM_bL_b$ at the junction A (Fig. 1) are derived considering the equilibrium condition on the each shell edge [3].

For the axisymmetric approximation, the edge loads acting on the representative cylindrical panel are the loads $\bar{Q}_{xo}$, $\bar{M}_{xo}$, and $\bar{N}_{xo}$ at the edge A. The edge load $\bar{N}_{xo}$ is taken to be

$$\overline{N}_{xo} = pR/2 \tag{2}$$

while the edge load $\overline{Q}_{xo}$, is calculated by considering the equilibrium of the cylindrical panel (Fig. 3). Thus

$$\int_{-\alpha}^{\alpha} \overline{Q}_{ox} \cos\theta R d\theta + 2pLR\sin\alpha - 2\sin\alpha \int N_\theta ds = 0 \tag{3}$$

where α is taken to be a small angle. The previous equation reduces to

$$\overline{Q}_{xo} R = \int N_\theta ds - pRL \tag{4}$$

Therefore, for the structure shown in Fig. 2

$$Q_{xm} R = \int_{AB_mC_m} N_\theta dx - pRL_m \tag{5a}$$

and

$$Q_{xb} r = \int_{AB_bC_b} N_\theta dx - prL_b \tag{5b}$$

Summing equations (5a) and (5b) and invoking (1) results in

$$Q_{xm} R + Q_{xb} r = pRr \tag{6}$$

For the continuity condition of the junction, the following conditions should be satisfied:

$$\varepsilon_{\theta m} = \varepsilon_{\theta b} \tag{7}$$

for the circumferential strain,

$$dw_b/dx = -dw_m/dX \tag{8}$$

for the rotation of normal,

$$M_{xb} = M_{xm} \tag{9}$$

for the bending moments.

Suitable expressions for N_{xm} and N_{xb} throughout the two shells are

$$N_{xm} = pR/2 \tag{10a}$$

$$N_{xb} = pr/2 \tag{10b}$$

It is to be noted that exact matching of stress resultants at the crotch point A would require that

$$N_{xm} = Q_{xb} \tag{10c}$$

$$N_{xb} = Q_{xm} \tag{10d}$$

However, since the stresses due to the axial stress resultants N_{xm} and N_{xb} at the crotch point are much smaller than the stresses due to the other stress resultants, the lack of enforcement of (10c) and (10d) in the analysis does not result in serious errors.

For different diameter and thickness intersecting pipe under internal pressure, the equations (6) to (10) should be also satisfied as shown in Fig. 4(a).

The KSHEL computer program [4] can analyze axisymmetric shell problems under symmetric loading not only elastically, but also in creep. With the following simplifying assumptions the KSHEL program can be also applied for a creep problem of tee branch pipe connection under internal pressure.

1. The pipes intersect normally.
2. The only external loading is that of uniform internal or external pressure.
3. The stress and strain distributions satisfy the thin shell assumptions; i.e., plane sections remain plane, transverse shear strains have negligible influence on the deformation, and transverse stresses have negligible influence on the shell mechanical behavior.
4. Circumferential bending strains are negligible in comparison with the circumferential direct strains.
5. Near the crotch stress gradients in the circumferential direction are small in comparison with stress gradients in the meridianal and thickness directions.

A special transformation matrix relating stress resultants and deformations between the edges of two different diameter cylinders is needed to enforce the equilibrium and the continuity conditions (Eqs. (6) to (10), refer to Fig. 4(b)).

The transfer matrix is derived as follows.

$$\begin{Bmatrix} Q_2 \\ N_2 \\ M_2 \\ W_2 \\ U_2 \\ \beta_2 \end{Bmatrix} = \begin{bmatrix} r/R & 0 & 0 & 0 & 0 & 0 \\ 0 & r/R & 0 & 0 & 0 & 0 \\ 0 & 0 & 1 & 0 & 0 & 0 \\ 0 & 0 & 0 & R/r & 0 & 0 \\ 0 & 0 & 0 & 0 & 1 & 0 \\ 0 & 0 & 0 & 0 & 0 & 1 \end{bmatrix} \begin{Bmatrix} Q_1 \\ N_1 \\ M_1 \\ W_1 \\ U_1 \\ \beta_1 \end{Bmatrix} + \begin{Bmatrix} -(\frac{R^2-r^2}{2R})p \\ -pr \\ 0 \\ 0 \\ 0 \\ 0 \end{Bmatrix} \quad (11)$$

The first element in the column matrix on the right can be simulated by "Ring Load" of $N_x = -(R^2-r^2)p/2r$ at the end of the branch pipe. The second can be simulated by "Ring Load" of $Q = pR$ at the end of the branch pipe.

The problem treated is one of determining the creep strains when they are small enough, so that thickness change may be neglected. By including in the model both elastic and creep strains, the analysis calculates the transient solution from the elastic stress distribution to the stationary state under steady internal pressure loading. The final creep solution of the stationary state represents the stress distribution over a significant portion of the life of the structure used in elevated temperature environment.

The governing equations for the deformation of an axisymmetric shell by nonlinear analysis are presented in [5]. Only the stress and strain equations should be changed to account for creep. Then the problem is solved by repeating steps in time. One such step, say from t_1 to t_2 will be described.

At t_1, the meridional and hoop stresses, σ_{x1} and $\sigma_{\theta 1}$, and the accumulated creep strains, ε_{cx1} and $\varepsilon_{c\theta 1}$, are known throughout the shell. The object is to find the total strains at time t_2. The total meridional and circumferential strains at t_2 are given by

$$\varepsilon_{x2} = A_{11}\sigma_{x2} + A_{12}\sigma_{\theta 2} + \varepsilon_{cx2} \tag{12a}$$

$$\varepsilon_{\theta 2} = A_{21}\sigma_{x2} + A_{22}\sigma_{\theta 2} + \varepsilon_{c\theta 2} \tag{12b}$$

where A_{11}, A_{12}, A_{21}, and A_{22} are some compliances, and the subscript c denotes the creep strain. For an elastic solution at the initial time, the compliances for an isotropic material are given by $A_{11} = A_{22} = 1/E$ and $A_{12} = A_{21} = -\nu/E$ where E is Young's Modulus and ν is Poisson's Ratio.

The accumulated creep strains at t_2 are given by the following equations [6].

$$\varepsilon_{cx2} = \varepsilon_{cx1} + \int_1^2 F_x(\sigma_x, \sigma_\theta)dt \tag{13a}$$

$$\varepsilon_{c\theta 2} = \varepsilon_{c\theta 1} + \int_1^2 F_\theta(\sigma_x, \sigma_\theta)dt \tag{13b}$$

Assuming a power creep law [7], with the exponent denoted by n, then the creep strain rates are given by

$$\dot{\varepsilon}_{cx} = F_x(\sigma_x, \sigma_\theta) = U_o \sigma_e^{n-1}(\sigma_x - \tfrac{1}{2}\sigma_\theta)/S_o^n \tag{14a}$$

$$\dot{\varepsilon}_{c\theta} = F_\theta(\sigma_x, \sigma_\theta) = U_o \sigma_e^{n-1}(\sigma_\theta - \tfrac{1}{2}\sigma_x)/S_o^n \tag{14b}$$

where U_o is the reference slope and S_o the reference stress of a standard reference creep curve, and

$$\sigma_e = (\sigma_x^2 + \sigma_\theta^2 - \sigma_x\sigma_\theta)^{\frac{1}{2}} \tag{15}$$

Penny and Marriott [8] present creep analyses in which F_x and F_θ in (14) are assumed constant based on the stresses that are evaluated at t_1. This simplifies the analysis, because then the integrand in (13) is independent of time and the creep strains at t_2 are given by

$$\varepsilon_{cx2} = \varepsilon_{cx1} + F_x(\sigma_{x1}, \sigma_{\theta 1})\Delta t \tag{16a}$$

$$\varepsilon_{c\theta 2} = \varepsilon_{c\theta 1} + F_\theta(\sigma_{x1}, \sigma_{\theta 1})\Delta t \tag{16b}$$

where $\Delta t = t_2 - t_1$. This means that then the elastic compliances A_{11} to A_{22} remain the same at all times, which makes the calculations simpler, but it means also that the creep strain that is accumulated during a time step is calculated on the basis of the creep strain rate at the beginning of the step.

Also, however, the present problem is different. Instead of the creep strain rates reaching a stationary state, they are expected to increase indefinitely at the critical time. For such problems, the simplified procedure was judged inadequate and the next level of approximation for the evaluation of the integral of (13) was used to obtain the results of this paper.

According to [9], the creep strain rates are expanded in a Taylor's series about the stresses at t_1

$$F_x(\sigma_x,\sigma_\theta) = F_x(\sigma_{x1},\sigma_{\theta 1}) + [\frac{\partial F_x}{\partial \sigma_x}]_1(\sigma_x-\sigma_{x1}) + [\frac{\partial F_{x1}}{\partial \sigma_\theta}]_1(\sigma_\theta-\sigma_{\theta 1}) \tag{17a}$$

$$F_\theta(\sigma_x,\sigma_\theta) = F_\theta(\sigma_{x1},\sigma_{\theta 1}) + [\frac{\partial F_\theta}{\partial \sigma_x}]_1(\sigma_x-\sigma_{x1}) + [\frac{\partial F_{\theta 1}}{\partial \sigma_\theta}]_1(\sigma_\theta-\sigma_{\theta 1}) \tag{17b}$$

and only the linear terms retained. The subscripts 1 mean that the derivatives are evaluated with the stresses at t_1. Also, the stresses at any time within the time step are

$$\sigma_x = \sigma_{x1} + (\sigma_{x2}-\sigma_{x1})(t-t_1)/\Delta t \tag{18a}$$

$$\sigma_\theta = \sigma_{\theta 1} + (\sigma_{\theta 2}-\sigma_{\theta 1})(t-t_1)/\Delta t \tag{18b}$$

Differentiating (14) as required by (17), substituting the stresses from (18), and then carrying out the integration in (13), gives the total strain at t_2 as

$$\varepsilon_{x2} = [A_{11} + \frac{\Delta t}{2}[\frac{\partial F_x}{\partial \sigma_x}]_1]\sigma_{x2} + [A_{21} + \frac{\Delta t}{2}[\frac{\partial F_x}{\partial \sigma_\theta}]_1]\sigma_{\theta 2}$$

$$+ \varepsilon_{cx1} + g_x \Delta t \tag{19a}$$

$$\varepsilon_{\theta 2} = [A_{21} + \frac{\Delta t}{2}[\frac{\partial F_\theta}{\partial \sigma_x}]_1]\sigma_{x2} + [A_{22} + \frac{\Delta t}{2}[\frac{\partial F_\theta}{\partial \sigma_\theta}]_1]\sigma_{\theta 2}$$

$$+ \varepsilon_{c\theta 1} + g_\theta \Delta t \tag{19b}$$

where

$$g_x = F_x(\sigma_{x1}, \sigma_{\theta 1}) - \frac{1}{2}[\frac{\partial F_x}{\partial \sigma_x}]\sigma_{x1} - \frac{1}{2}[\frac{\partial F_x}{\partial \sigma_\theta}]_1 \sigma_{\theta 1} \tag{20a}$$

$$g_\theta = F_\theta(\sigma_{x1}, \sigma_{\theta 1}) - \frac{1}{2}[\frac{\partial F_\theta}{\partial \sigma_x}]\sigma_{x_1} - \frac{1}{2}[\frac{\partial F_\theta}{\partial \sigma_\theta}]_1 \sigma_{\theta 1} \tag{20b}$$

This approximation for the integration of the creep strain rate is used by one option of the KSHEL program.

This level of approximation does take more computer time per time step than the simplified approach that would use (16), because the elastic constants A_{11} to A_{22}, must be recalculated at every time step. However, the higher level approximation will require fewer time steps, in order to achieve adequate accuracy, and in the end may require less total computer time, than the simpler approach.

Then, constitutive relations which include both elastic strains and power-law creep strains in a thin axisymmetric shell of isotropic material are

$$\dot{\varepsilon}_x = (\dot{\sigma}_x - \nu\,\dot{\sigma}_\theta)/E + U_o \sigma_e^{n-1}(\sigma_x - \sigma_\theta/2)/S_o^n \tag{21a}$$

$$\dot{\varepsilon}_\theta = (\dot{\sigma}_\theta - \nu\,\dot{\sigma}_x)/E + U_o \sigma_e^{n-1}(\sigma_\theta - \sigma_x/2)/S_o^n \tag{21b}$$

Dots over the variables indicate differentiation with respect to the pseudo-time variable τ of a time hardening creep theory.

Thus, for the present study the function F_x and F_θ are given

$$F_x = U_o\, \sigma_e^{n-1}(\sigma_x - \sigma_\theta/2)/S_o^n \tag{22a}$$

$$F_\theta = U_o\, \sigma_e^{n-1}(\sigma_\theta - \sigma_x/2)/S_o^n \tag{22b}$$

III. ANALYSIS

The analysis model presented here can be applied to many tee branch pipe connections. Any combination of thickness, radius and material properties between a main and branch pipe is available if a combination satisfies the five assumptions in chapter II.

As typical cases, the following three cases, which have the ratio of the branch pipe radius to the main pipe radius equal to 0.5 (r/R=0.5), are analyzed.

1. Case of equal strength between both pipes
   (denoted as s/S = 1)
2. Case of equal thickness between both pipes
   (denoted as t/T = 1)
3. Opening compensation of No. 1; the main pipe is reinforced. (See Appendix II)
   (denoted as OPNC)

In Table 1, the structural dimensions and the mechanical properties of the material of the above three cases are shown. Calculations of the required reinforcement for case 3 according to the ASME code [10] and the resulting thickness profile are presented in Appendix II.

Prior to the analysis of the three cases some sample analyses were performed to check the validity of the proposed model. In

Appendix I the results of the sampel analyses are shown. It is concluded as a result of the study of the sample analyses that the developed transfer matrix works as expected and the presented model is valid in any combination of normally intersecting cylindrical pipes under internal pressure.

IV. RESULTS AND DISCUSSION

First of all the case of s/S = 1 is discussed. For the other cases, discussions will be presented later.

Case of s/S=1

The maximum dimensionless equivalent stress versus the dimensionless pseudo-time parameter is given in Fig. 5. The ratio of the maximum equivalent stress σ_e to the nominal stress pR/T of the main pipe reaches the asymptotic value of 7.82 which occurs on the outside surface of the branch pipe at the crotch.

Nondimensional stresses at the crotch point when the stationary state is reached are given in Table 2. In this table, the elastic solution which is the first step solution of the creep calculation is also given. The maximum stress occurs on the outside of the branch pipe in both cases of elastic and stationary state. The maximum elastic stress reduces to approximately sixty-seven percent in the stationary state due to stress redistribution.

The dimensionless axial moment $(6M_x/Tt)(T/pR)$ distribution along the meridianal direction is presented in Fig. 6. In both cases of elastic and stationary state, the moment equilibrium are satisfied at the crotch point. The maximum moment occurs at the crotch point in the branch and the point of $x/\sqrt{RT}$ is around one (1) in the main respectively. This suggests that the maximum meridianal bending stresses will occur at these points.

Fig. 7 shows the dimensionless circumferential stress resultant N_θ/pR, N_θ/pr distribution along the pipe axis. The distributions satisfy Eq. (1) in both elastic and stationary creep solution. The ratio of N_θ to product of the internal pressure p and the each radius of pipe (r,R) reaches to one (1) in the region of remote from the crotch. The dimensionless stress distributions along the pipe axis are shown in Fig. 8 to Fig. 11. Fig. 8 and Fig. 9 shows the meridional direction stress distribution on inside and outside surfaces respectively.

As discussed in Fig. 6, it is clear that the maximum meridianal bending stress occurs at the crotch. The circumferential stress distributions are given in Fig. 10 and Fig. 11.

Fig. 12 shows the distributions of the dimensionless stationary state strain rate in circumferential and thickness directions along the pipe axis. The stationary creep rate in the thickness direction may be determined from the incompressibility condition

$$\dot{\varepsilon}_z = - (\dot{\varepsilon}_x + \dot{\varepsilon}_\theta) \qquad (23)$$

Since in shell theory the strain rates $\dot{\varepsilon}_x$ and $\dot{\varepsilon}_\theta$ vary linearly with thickness coordinate, the thickness average creep rates are simply the arithmetric means of the value at the inner and outer surfaces of the shell. In the following discussion, the symbol $\dot{\varepsilon}_z$ will refer to the average value.

The $\dot{\varepsilon}_\theta$ in the branch has the maximum value near the crotch, which is greater than the maximum thickness direction strain rates and the $\dot{\varepsilon}_\theta$ in the main. Also, Fig. 12 shows that the thickness of the branch reduces faster than the main by approximately 1.4 times and the creep rupture due to creep deformation would occur on the branch side of the crotch point.

The $\dot{\varepsilon}_\theta$ and $\dot{\varepsilon}_z$ calculated from the elastic solution are also shown in parentheses in Table 3. The elastically calculated strain rates are more than two times and five times in the main and branch, respectively, than the stationary state strain rates.

Case of t/T=1

The normalized stresses at the crotch point are given in Table 2. The stress values in the main and branch are almost the same. This is apparent from the dimensional reasoning; the ratio of each pipe r/R is 0.5 and the ratio of each thickness t/T is 1.0. These stresses are almost half or less than those of the case of s/S=1. From the strength design point such stress condition is preferable to the case of s/S=1. The stationary state strain rates are reduced, especially at the branch the thickness direction strain rates reduces to approximately twenty percent of the case of s/S=1 as shown in Table 3. In Fig. 13 and Fig. 14 the dimensionless stationary strain rate distribution is shown

in the circumferential and the thickness direction respectively. These figures indicate that in the case of equal thickness a symmetric creep deformation to the crotch point will be expected in the both pipes.

The elastically calculated stationary strain rates are shown in Table 3. The strain rates in both pipes are more than three times as large as the stationary state strain rates.

Case of OPNC

In this case, it is expected that the reinforcement in the main reduces the branch stresses and strain rate of the s/S=1. The normalized stresses and the strain rates in stationary state are shown in Table 2 and Table 3 respectively. The strain rates are greatly reduced from those of the case of s/S=1, and the reduction rate is ninety percent in the circumferential direction and eighty percent in the thickness direction of the branch. Such large reductions can not be expected even in the case of t/T=1. The stationary state stress distributions are shown in Fig. 8 to Fig. 11 for this case with the case of s/S=1 for comparison. These figures indicate that the reinforcement reduces not only the stresses in the branch greatly but also the stresses in the main itself within the reinforcing zone.

A main reason for the reduction of the stresses and the strain rates are considered as follows.

Due to the reinforcement in the main around the crotch point, the radial and the circumferential deformation of the main is much more restrained than the case of s/S=1.

In Fig. 6 the crotch point stationary state bending moments are shown for the both cases of OPNC and t/T=1 for a comparison. From this comparison it is clear that a reinforcement in the main reduces the bending moment to less than half but a reinforcement in the branch the moment reduction is much less. This is reasonable from the discussion just before. It seems that in the case of t/T=1 the increased rigidity of the branch produces larger bending moment than do the other two cases to make the continuity condition at the crotch.

Therefore, from the foregoing discussion it is concluded that in a tee branch connection a reinforcement in a main pipe will reduce stresses and stationary state strain rates more than reinforcement in a branch pipe.

The elastically calculated strain rates are shown in Table 3. The strain rates are more than two times and six times in the main and branch respectively than the stationary strain rates.

V. CONCLUSIONS

An axisymmetric replacement model has been developed to describe the creep behavior in the crotch region of different diameter and thickness intersecting pipes under internal pressure. Three kinds of typical tee branch connections were analyzed by the model. The model predicts that significant redistribution of stress takes place in this region, as the creep strains increase from the initial zero value to values of elastic order. Therefore, predictions of the creep life on the basis of stresses calculated by elastic analysis would be too conservative in the case of materials following a highly nonlinear creep law.

An effect of reinforcement of hole was examined. The reinforcement according to the ASME code reduced the creep strain rates significantly in the studied case.

For a design purpose, equal thickness in both pipes or a reinforcement in a main pipe would be recommended rather than a design of equal strength in both pipes. A reinforcement in a main pipe reduces stresses and strain rates much more than in the case of equal thickness.

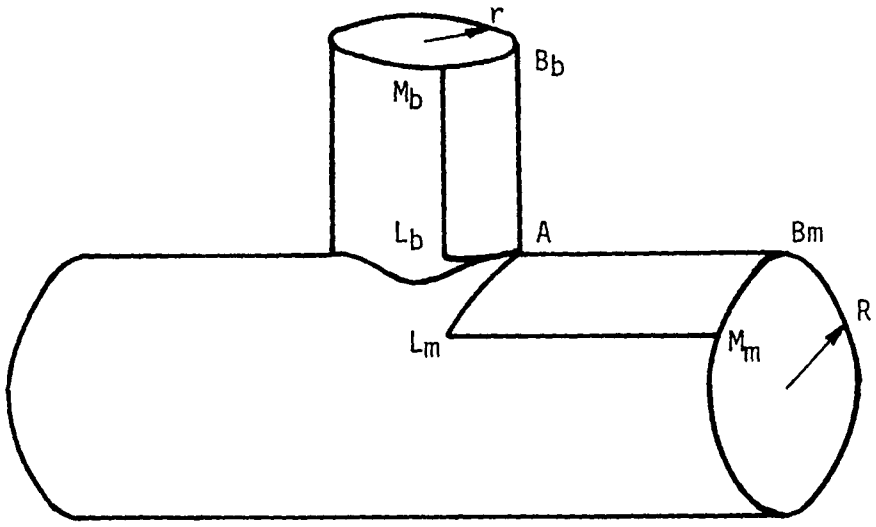

(a)

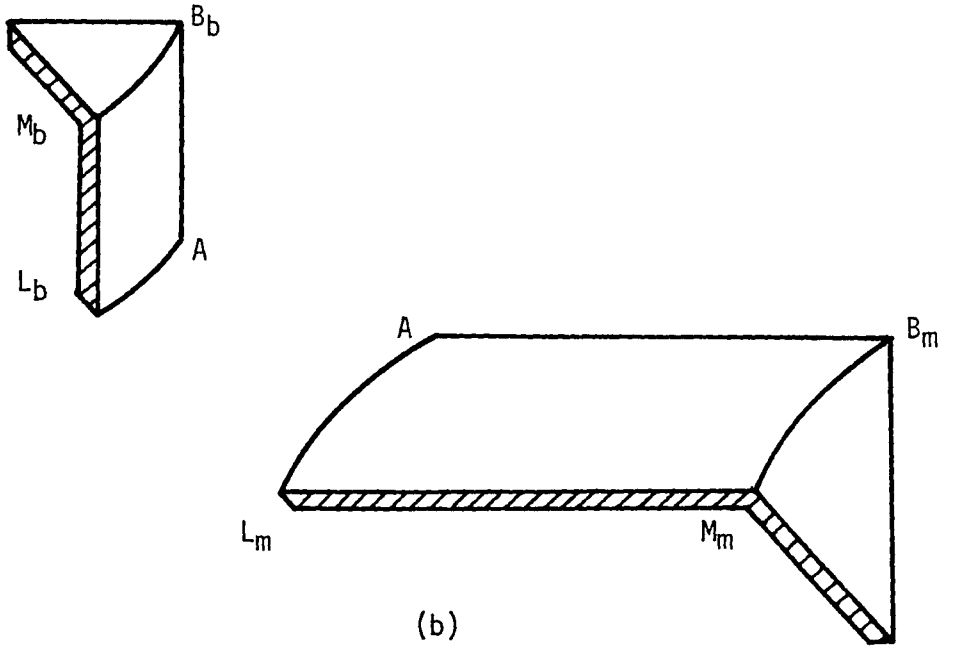

(b)

Fig. 1(a) Tee Branch Connection
1(b) Representative Cylindrical Panels

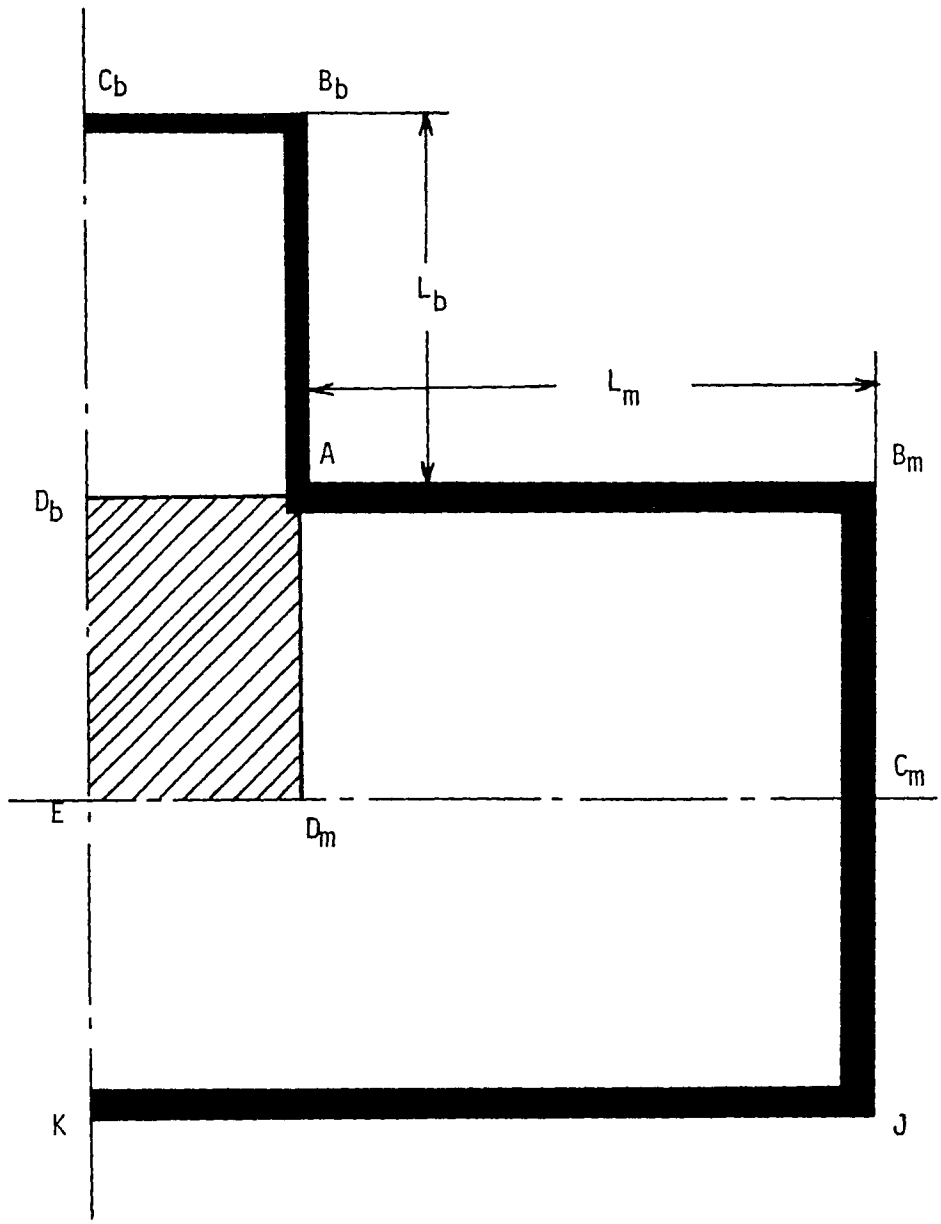

Fig. 2. Section used for Calculating Forces in the Overall Equilibrium Equation

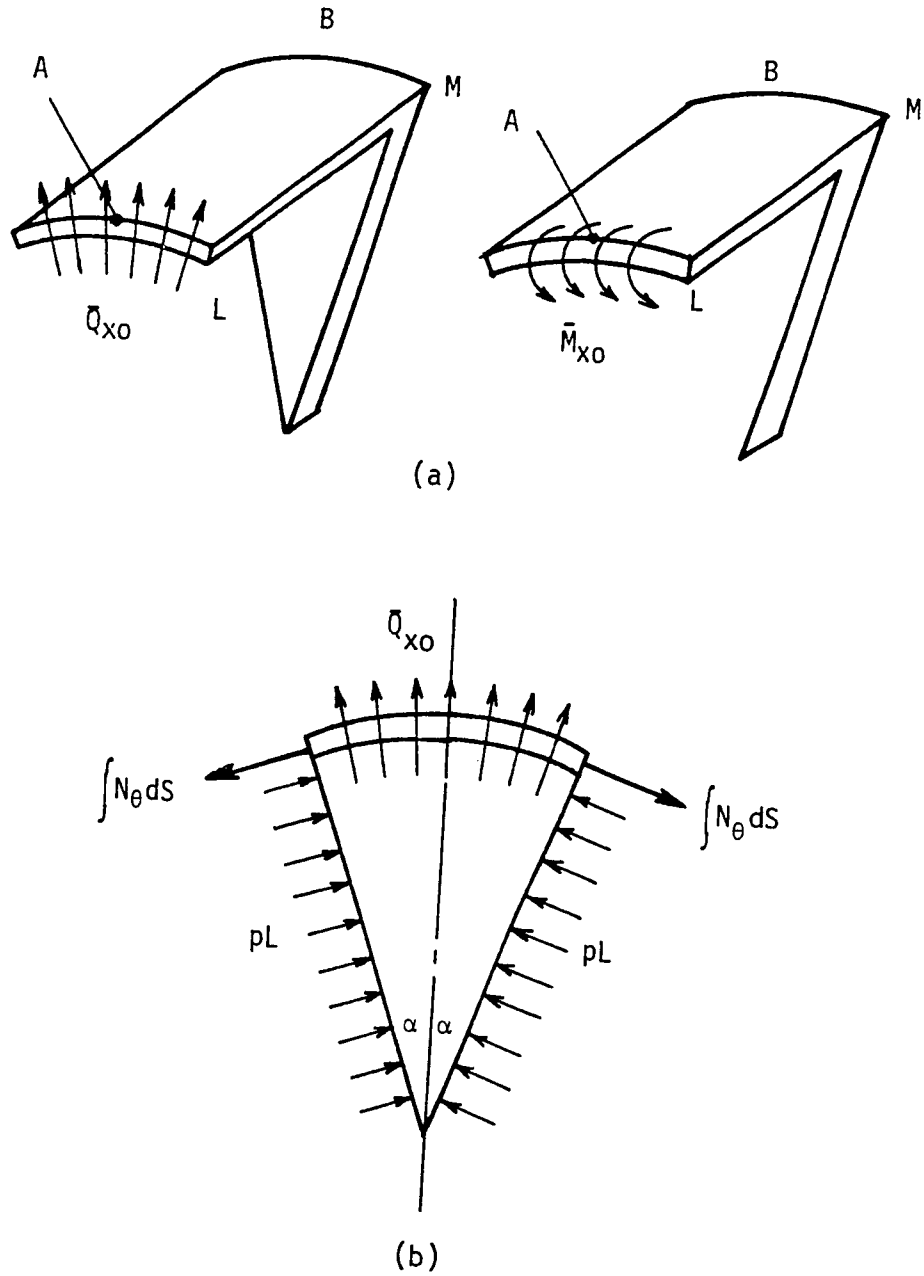

Fig. 3. Edge Loads and Equilibrium of Representative Cylindrical Panel

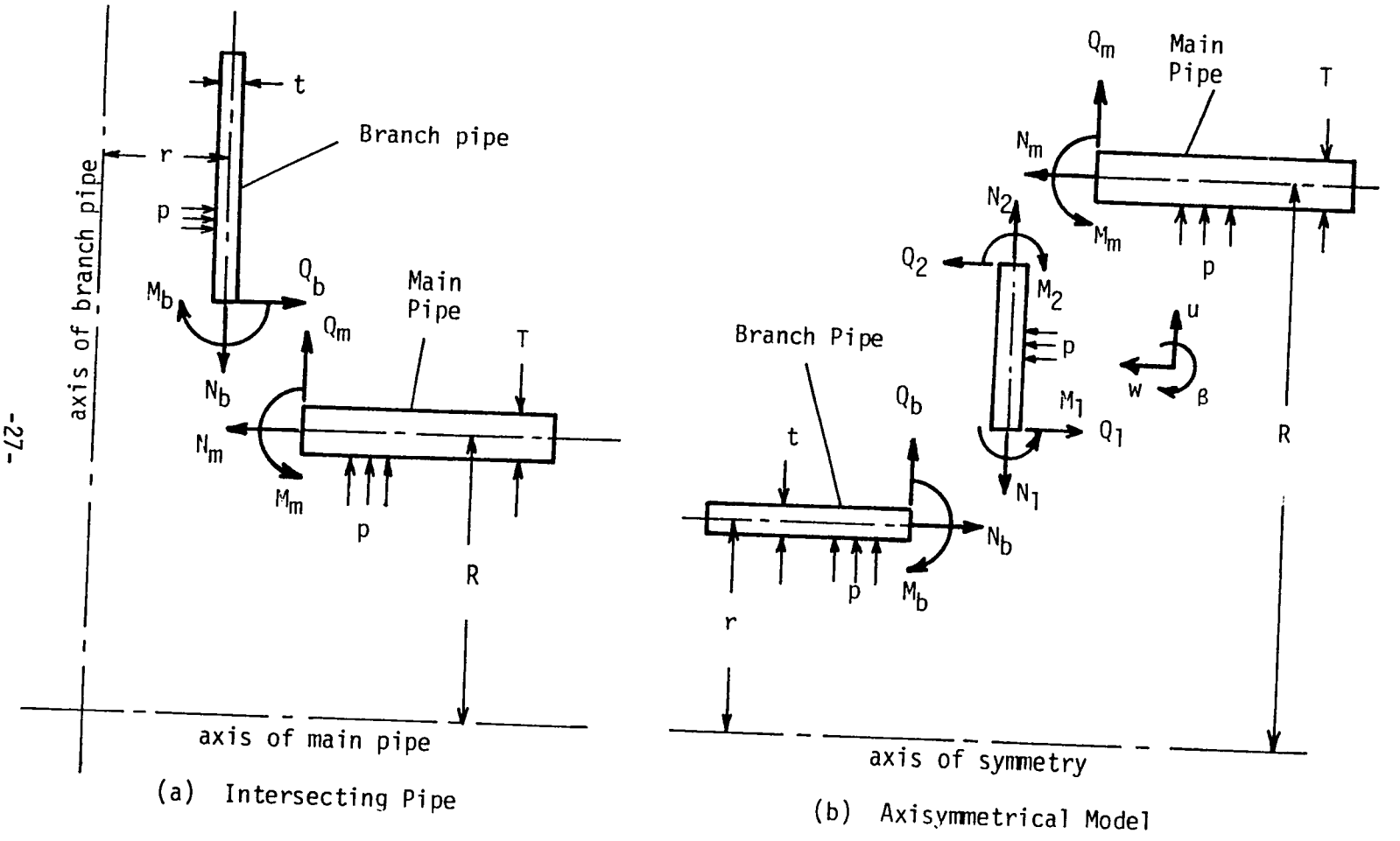

Fig. 4. Modeling of Intersecting Pipe

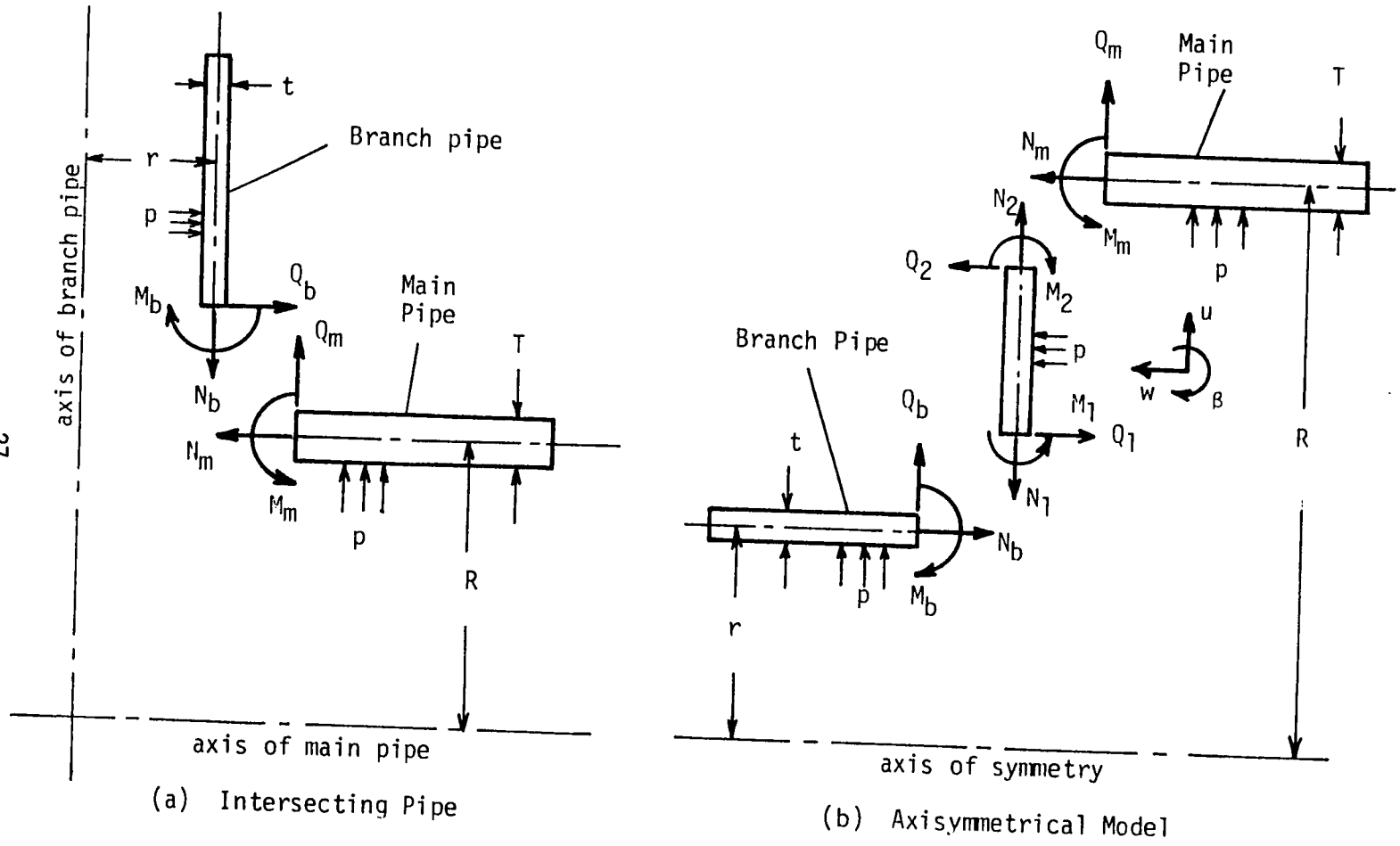

Fig. 4. Modeling of Intersecting Pipe

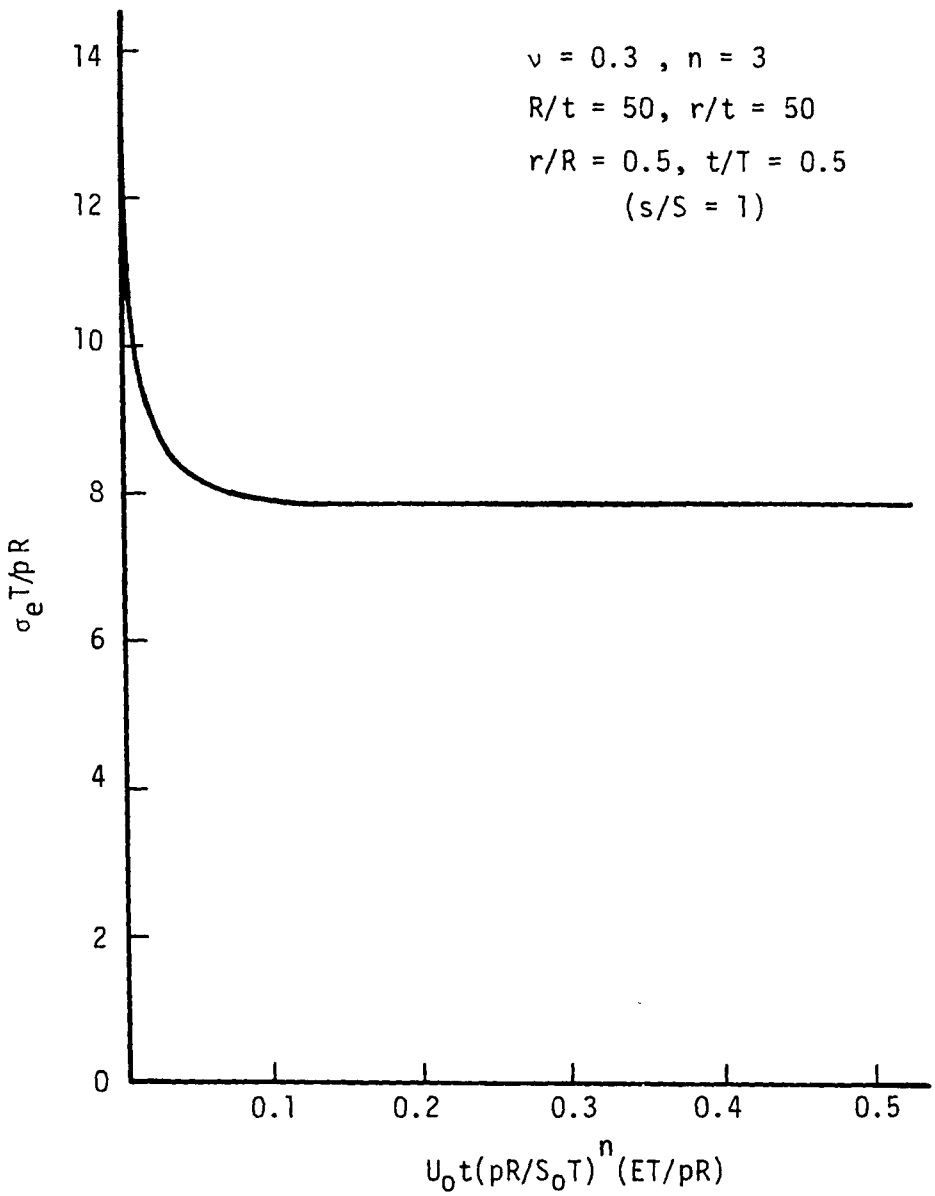

Fig. 5. Dimensionless Equivalent Stress At Crotch Point Versus a Dimensionless Time Parameter.

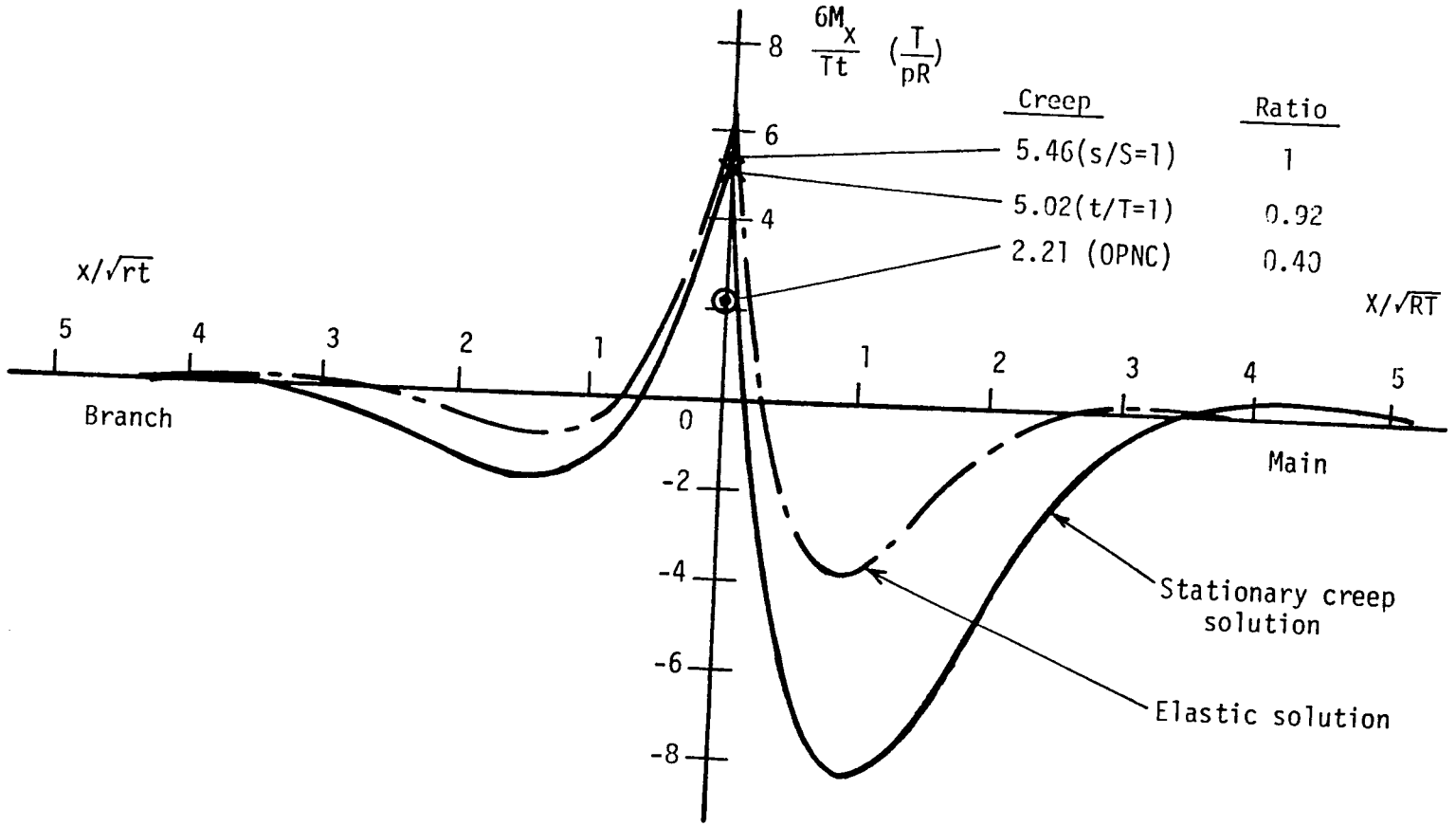

Fig. 6. $(6M_x/Tt)(T/pR)$ versus $X/\sqrt{RT}$, $x/\sqrt{rt}$

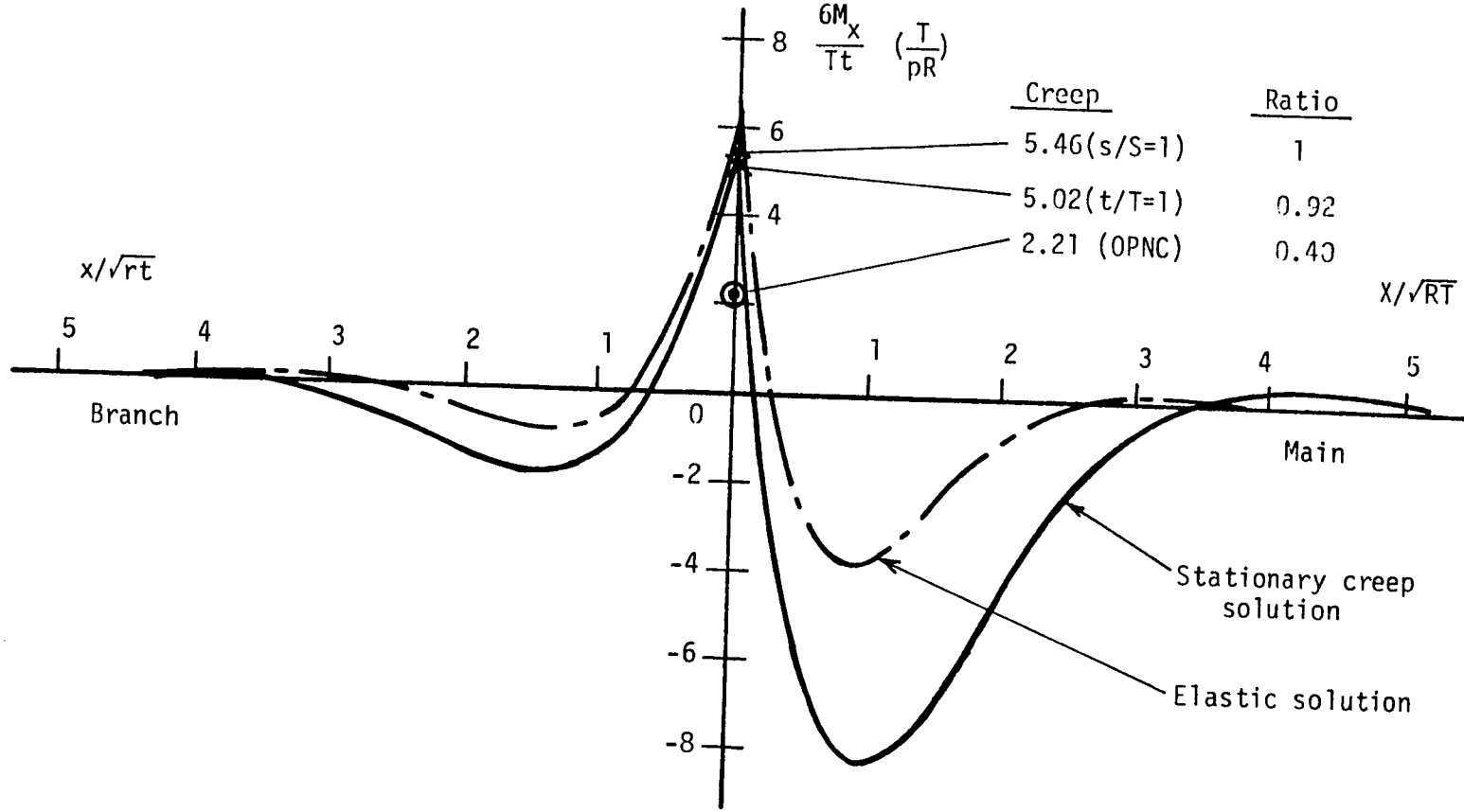

Fig. 6. $(6M_x/Tt)(T/pR)$ versus $X/\sqrt{RT}$, $x/\sqrt{rt}$

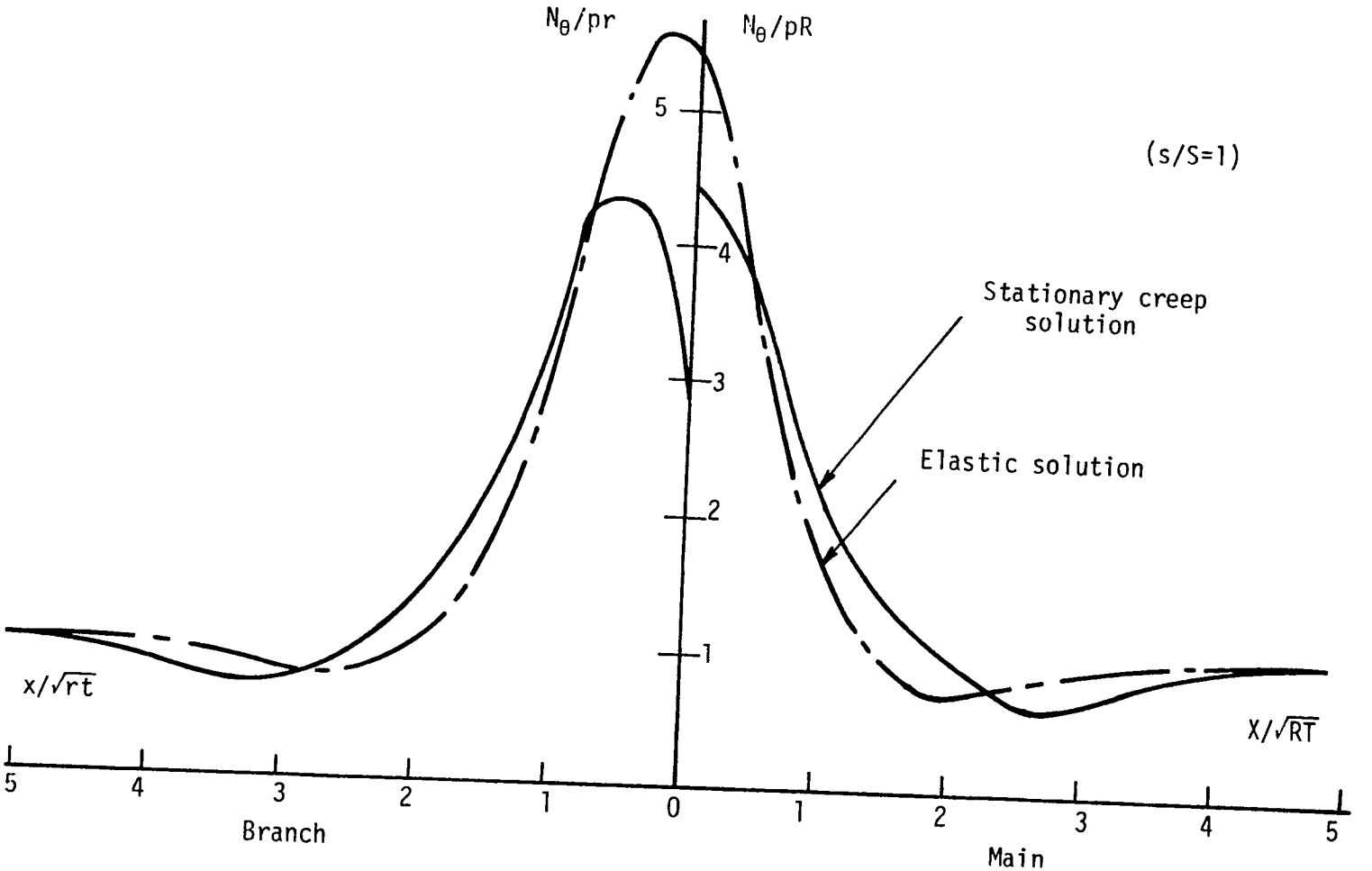

Fig. 7. N_θ/pR versus $X/\sqrt{RT}$ and N_θ/pr versus $x/\sqrt{rt}$

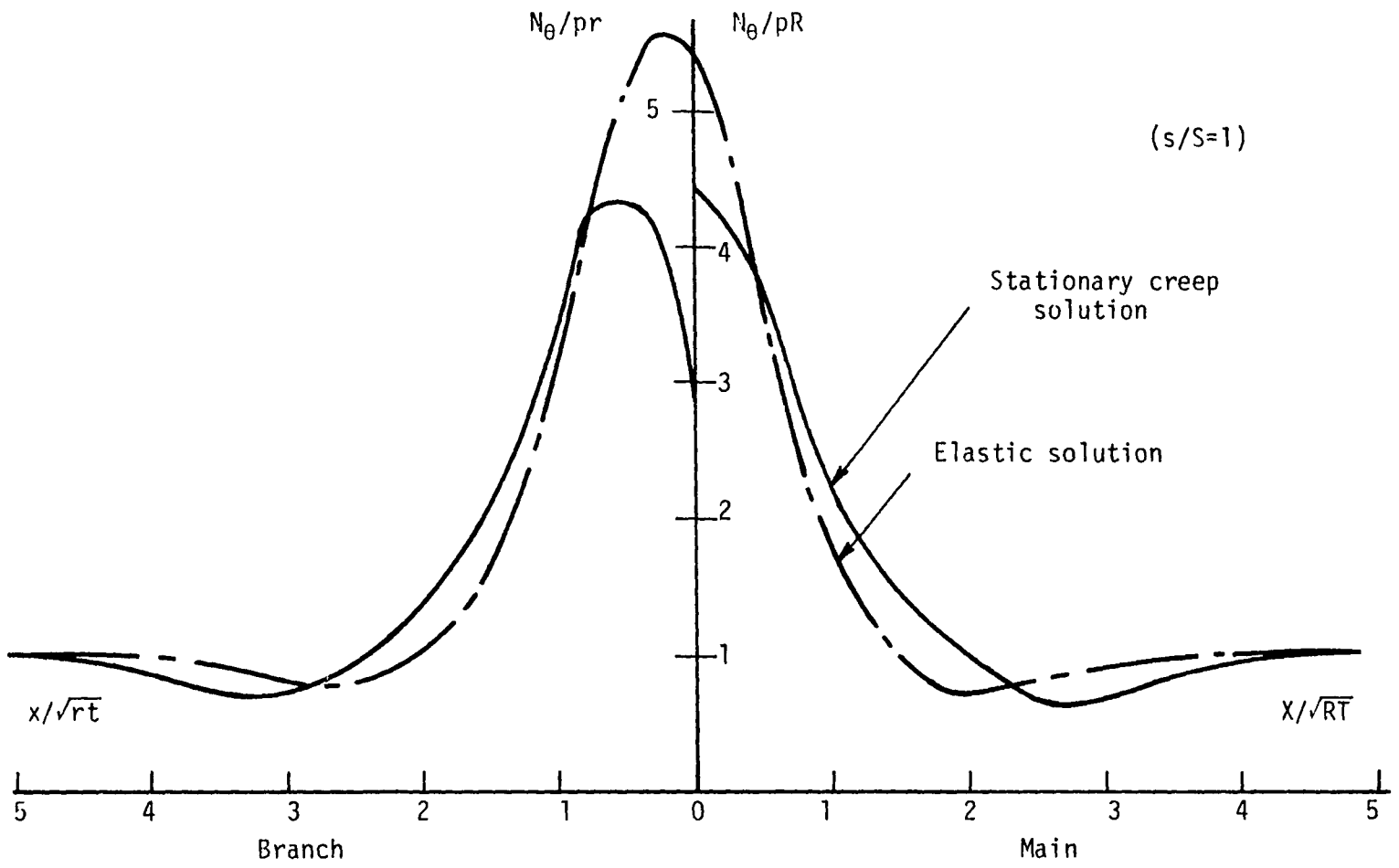

Fig. 7. N_θ/pR versus $X/\sqrt{RT}$ and N_θ/pr versus $x/\sqrt{rt}$

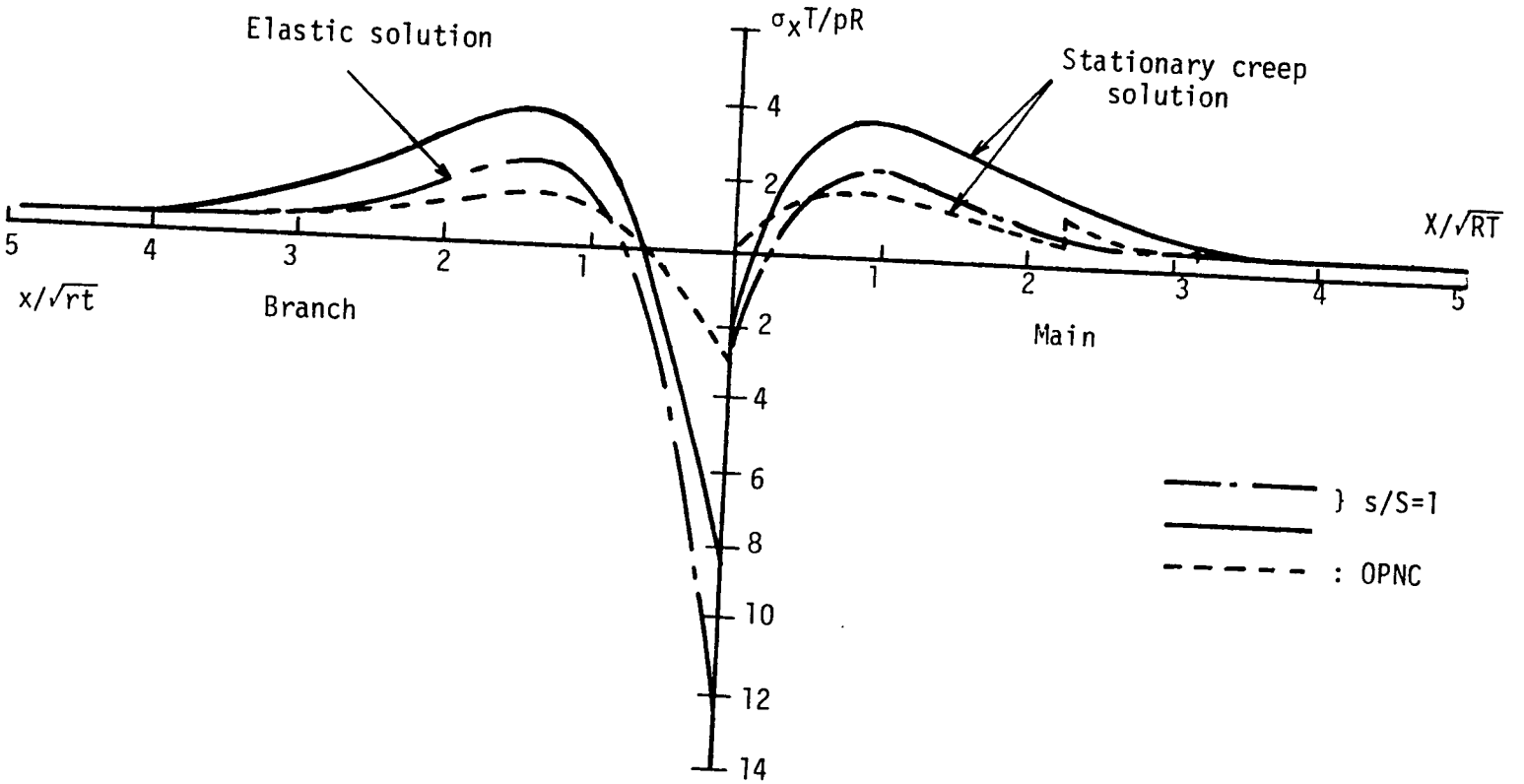

Fig. 8. Axial Stress on Inside Surface

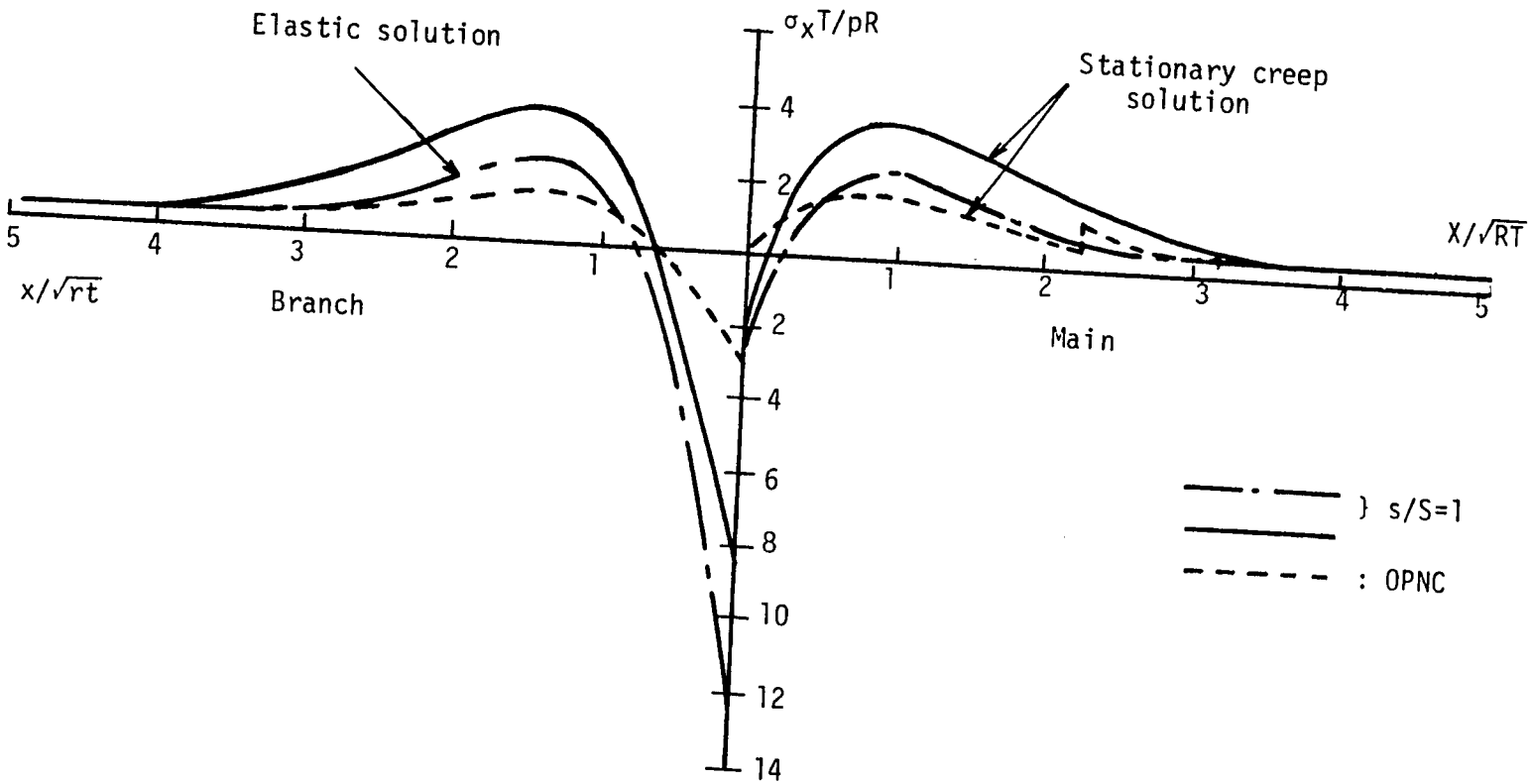

Fig. 8. Axial Stress on Inside Surface

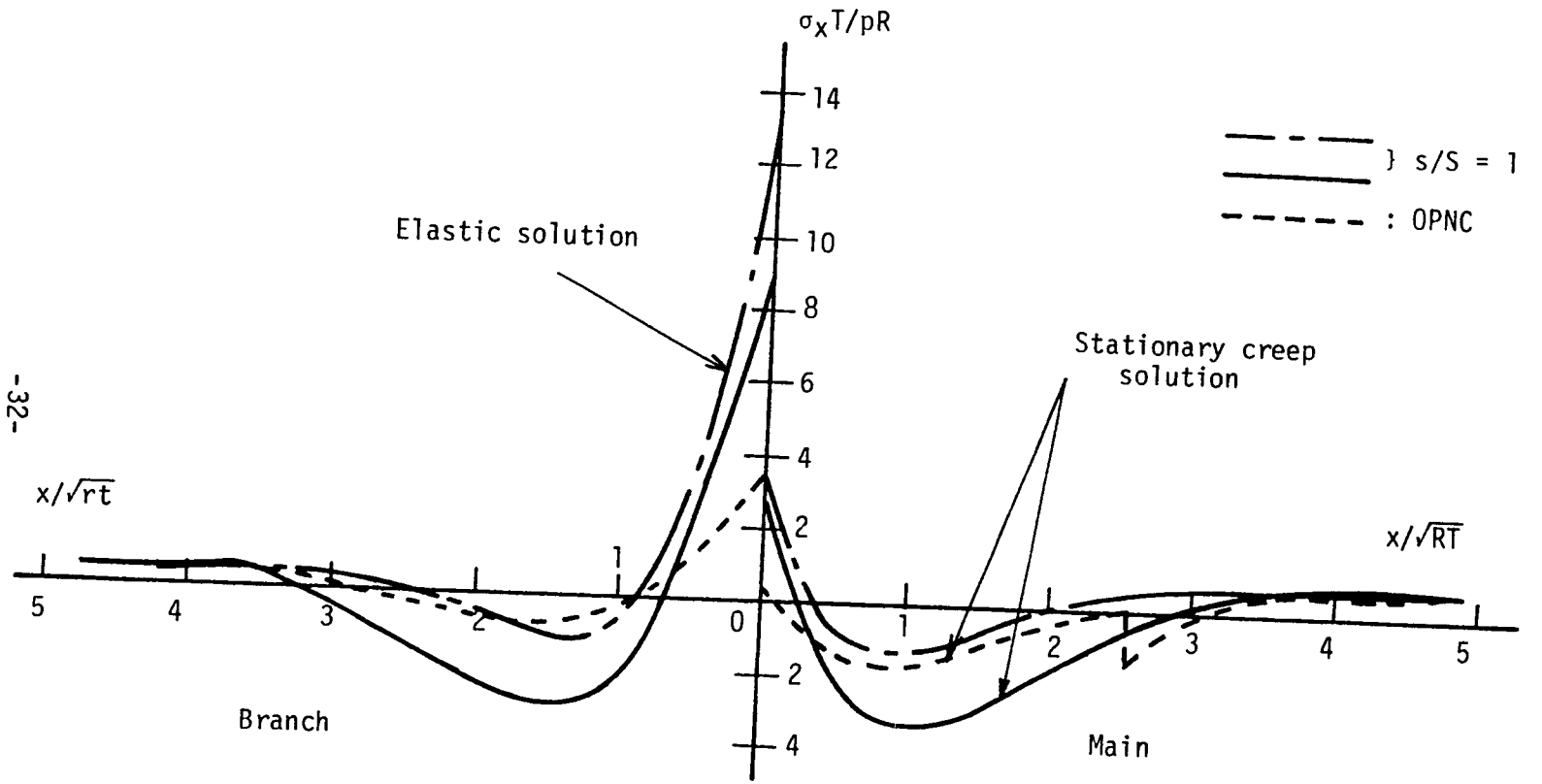

Fig. 9. Axial Stress on Outside Surface

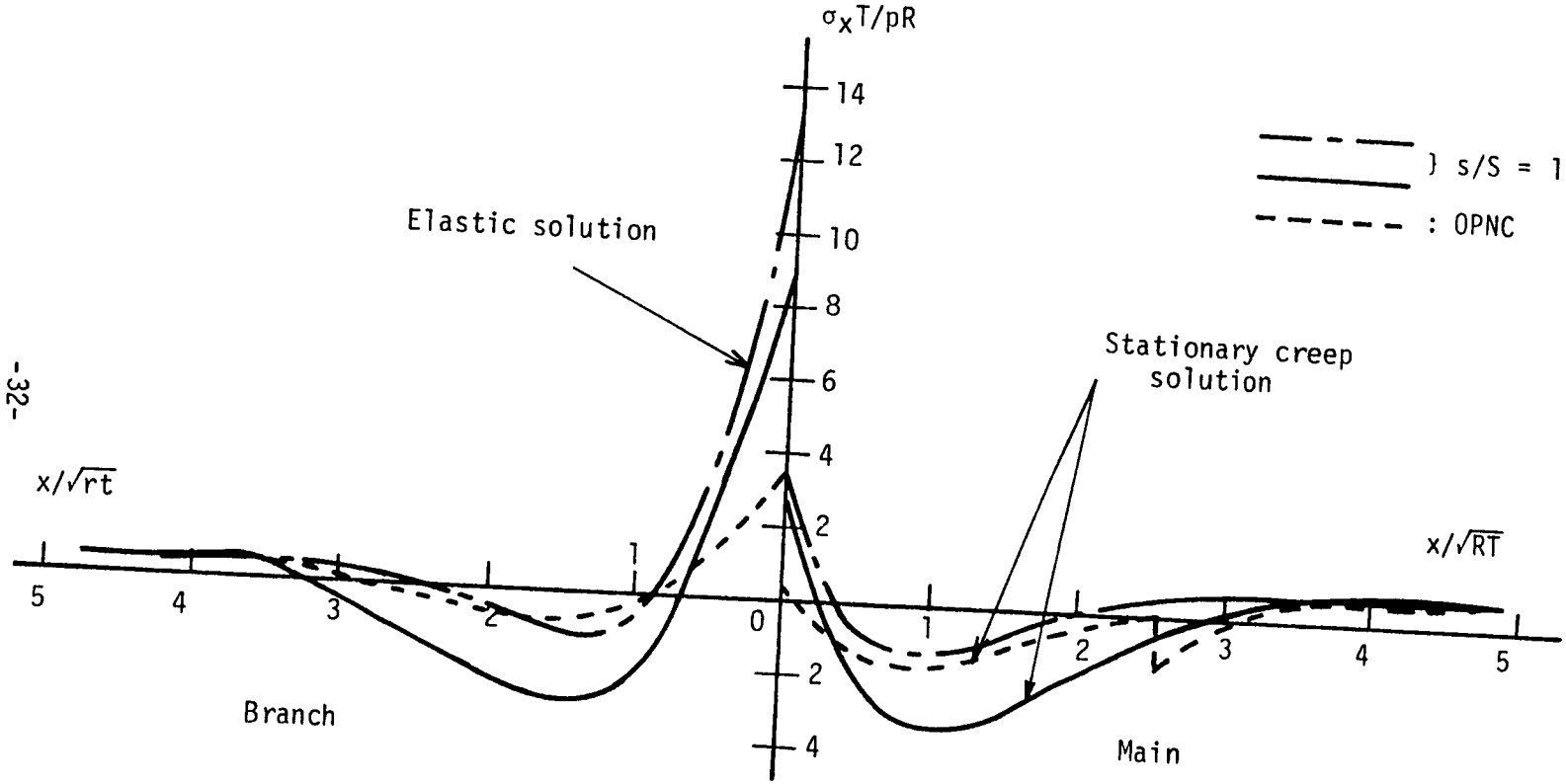

Fig. 9. Axial Stress on Outside Surface

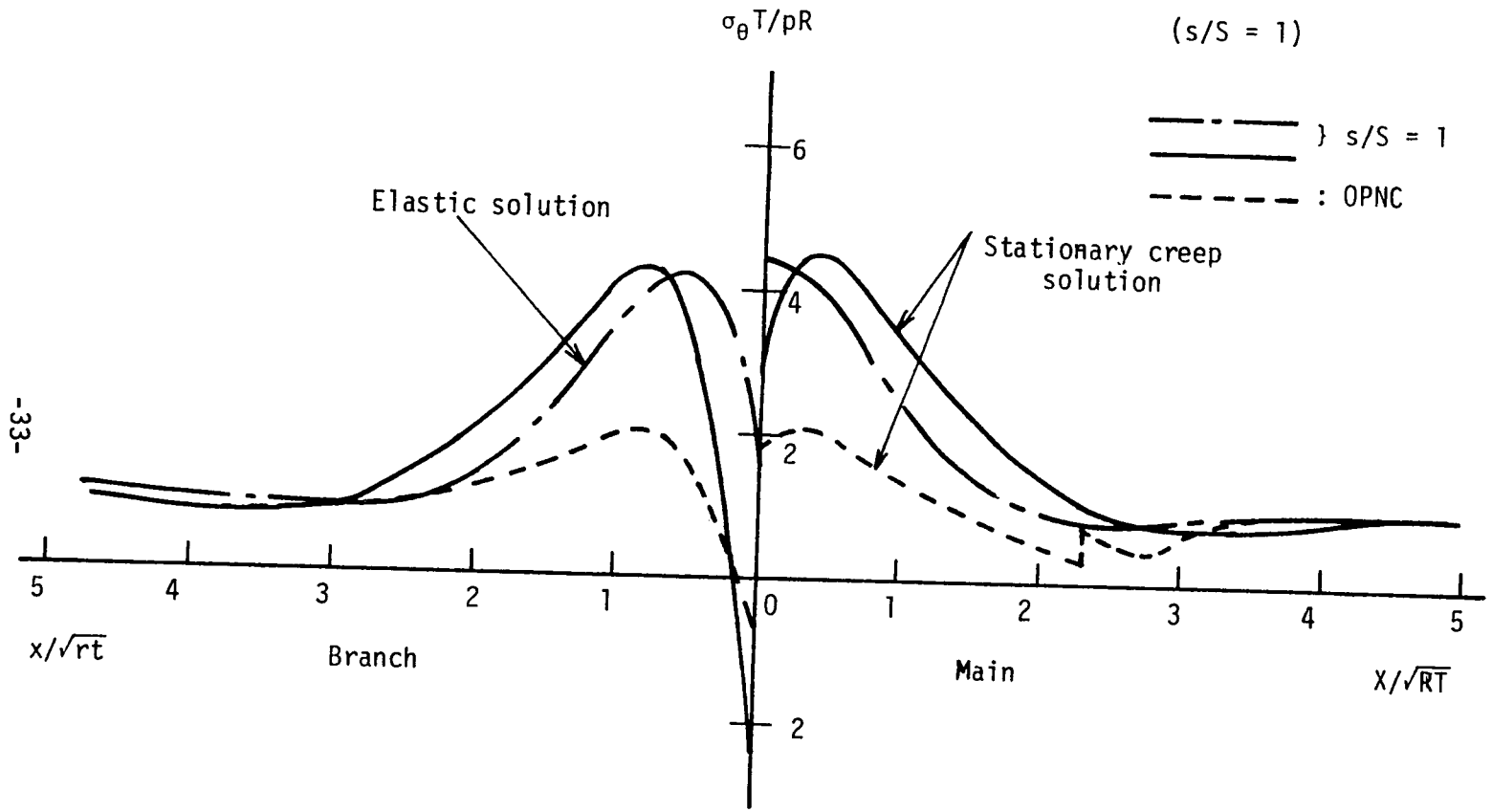

Fig. 10. Circumferential Stress on Inside Surface

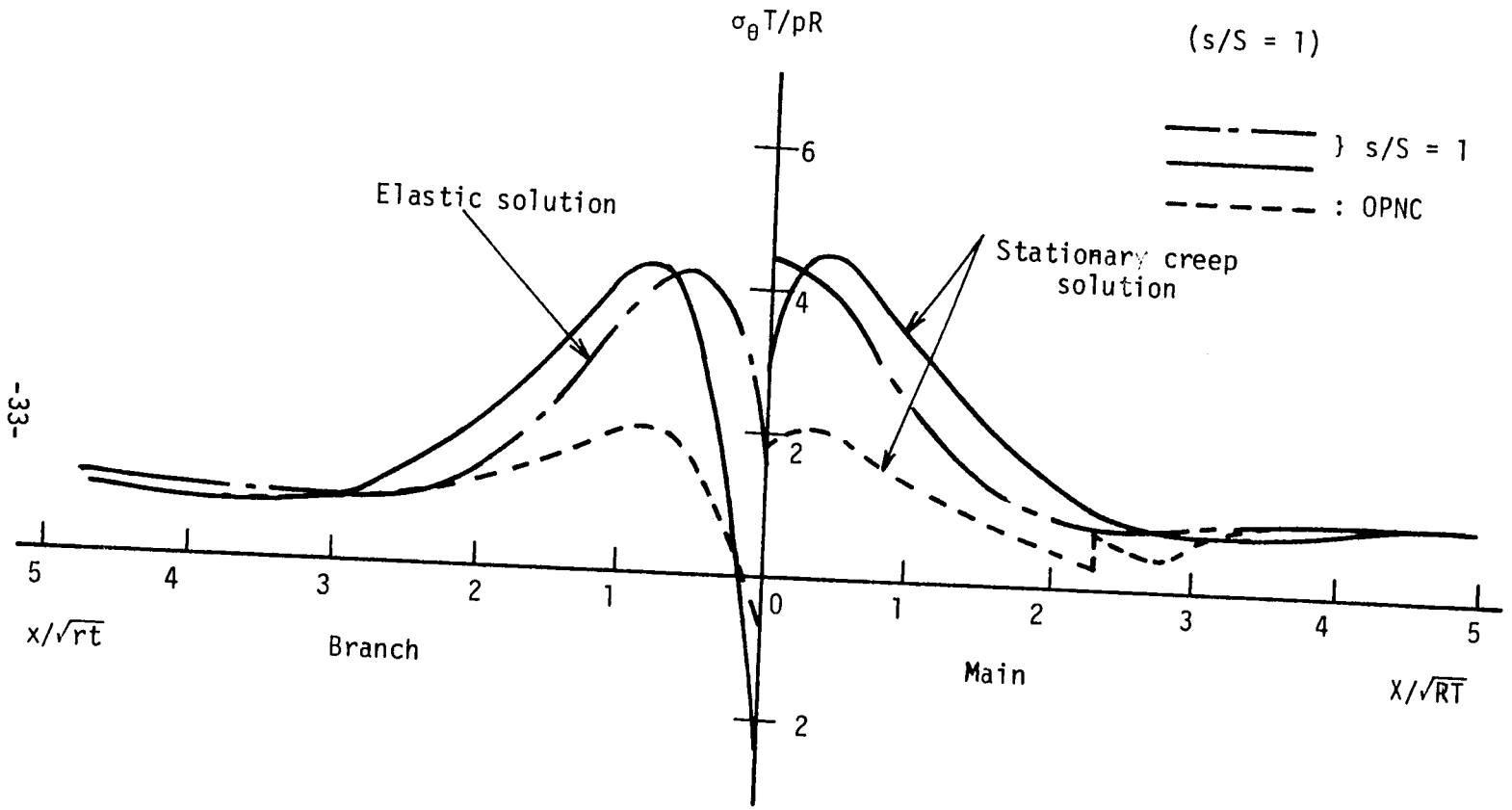

Fig. 10. Circumferential Stress on Inside Surface

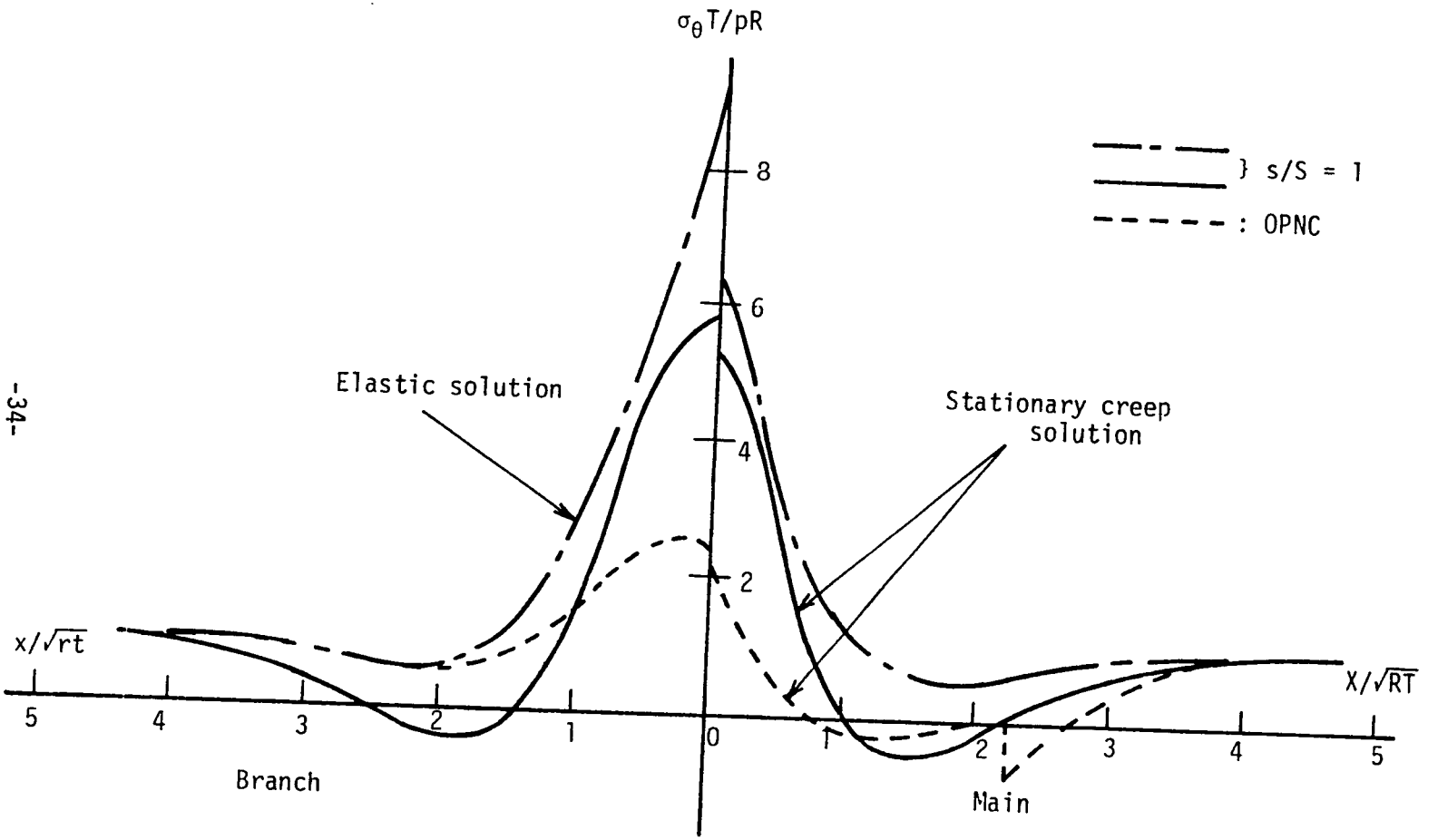

Fig. 11. Circumferential Stress on Outside Surface

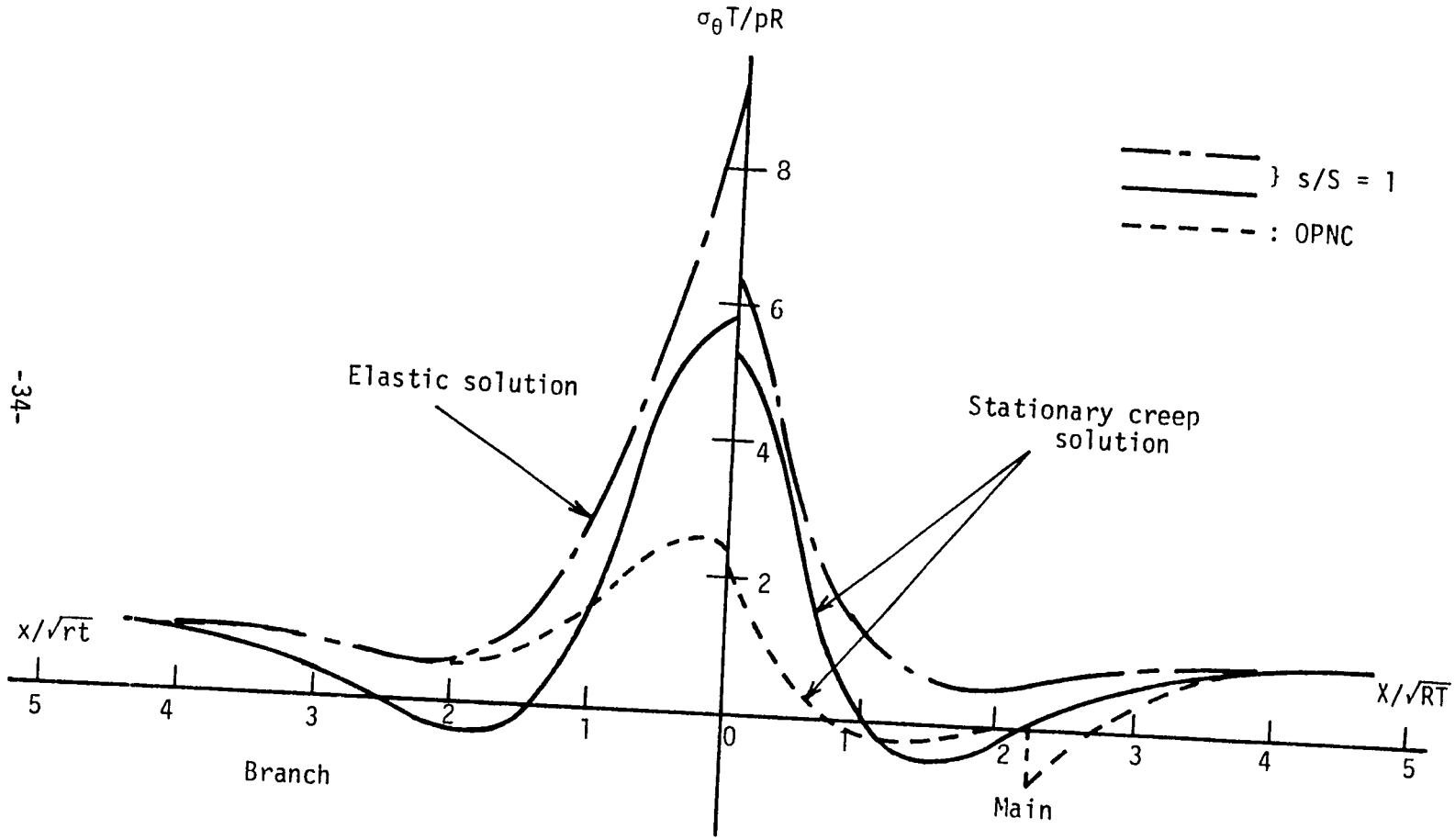

Fig. 11. Circumferential Stress on Outside Surface

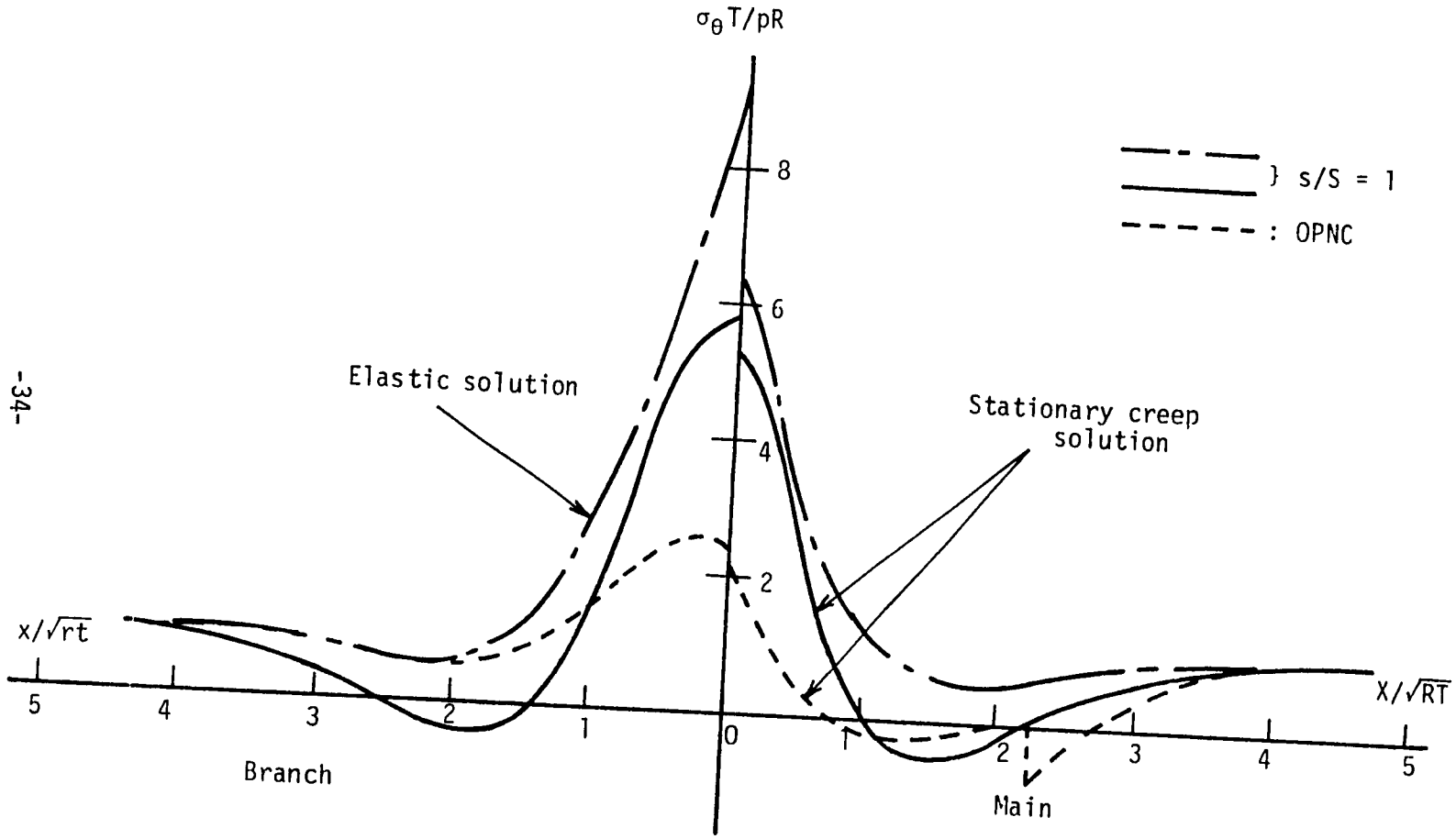

Fig. 11. Circumferential Stress on Outside Surface

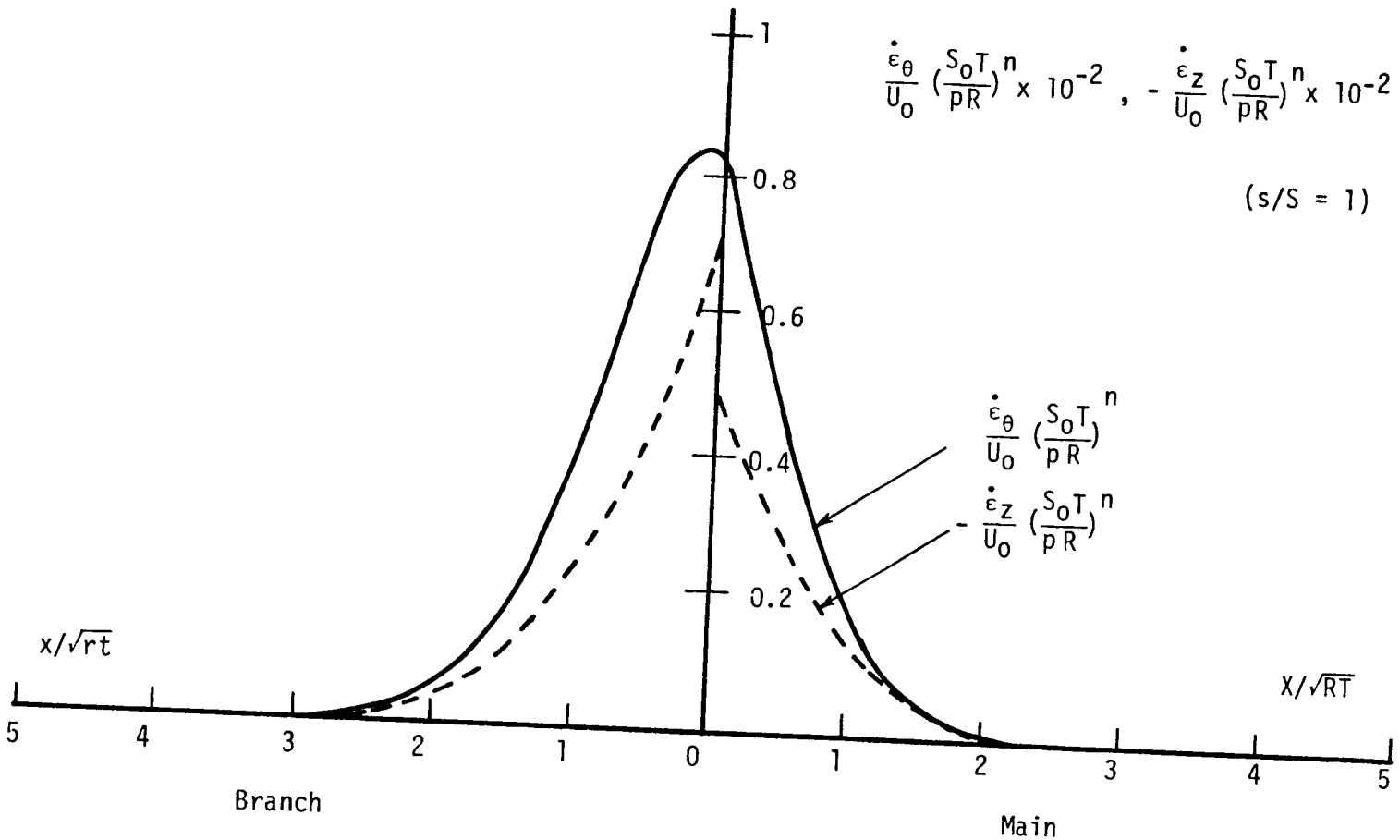

Fig. 12. Dimensionless Stationary Creep Strain Rate Along Pipe Axis

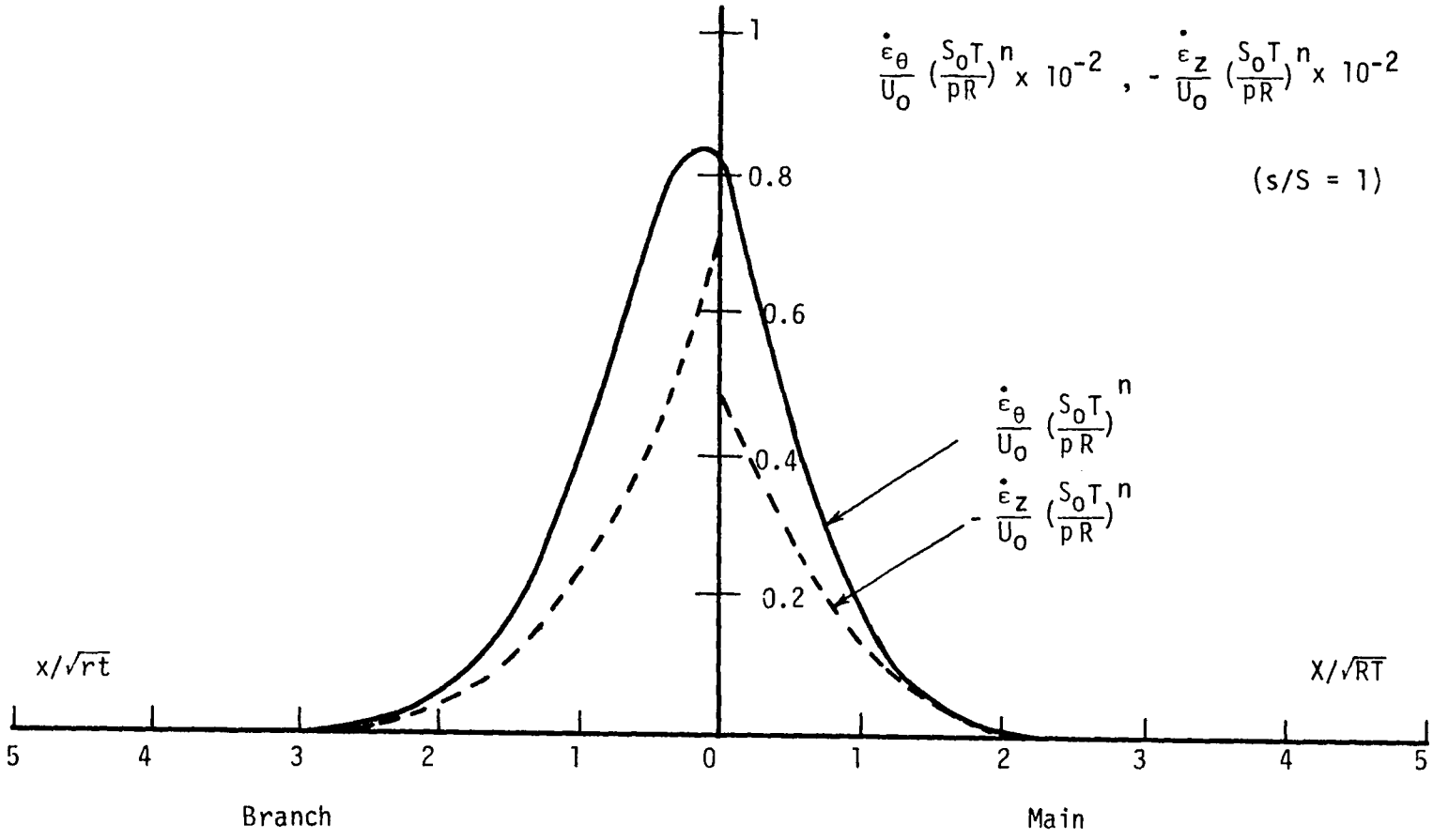

Fig. 12. Dimensionless Stationary Creep Strain Rate Along Pipe Axis

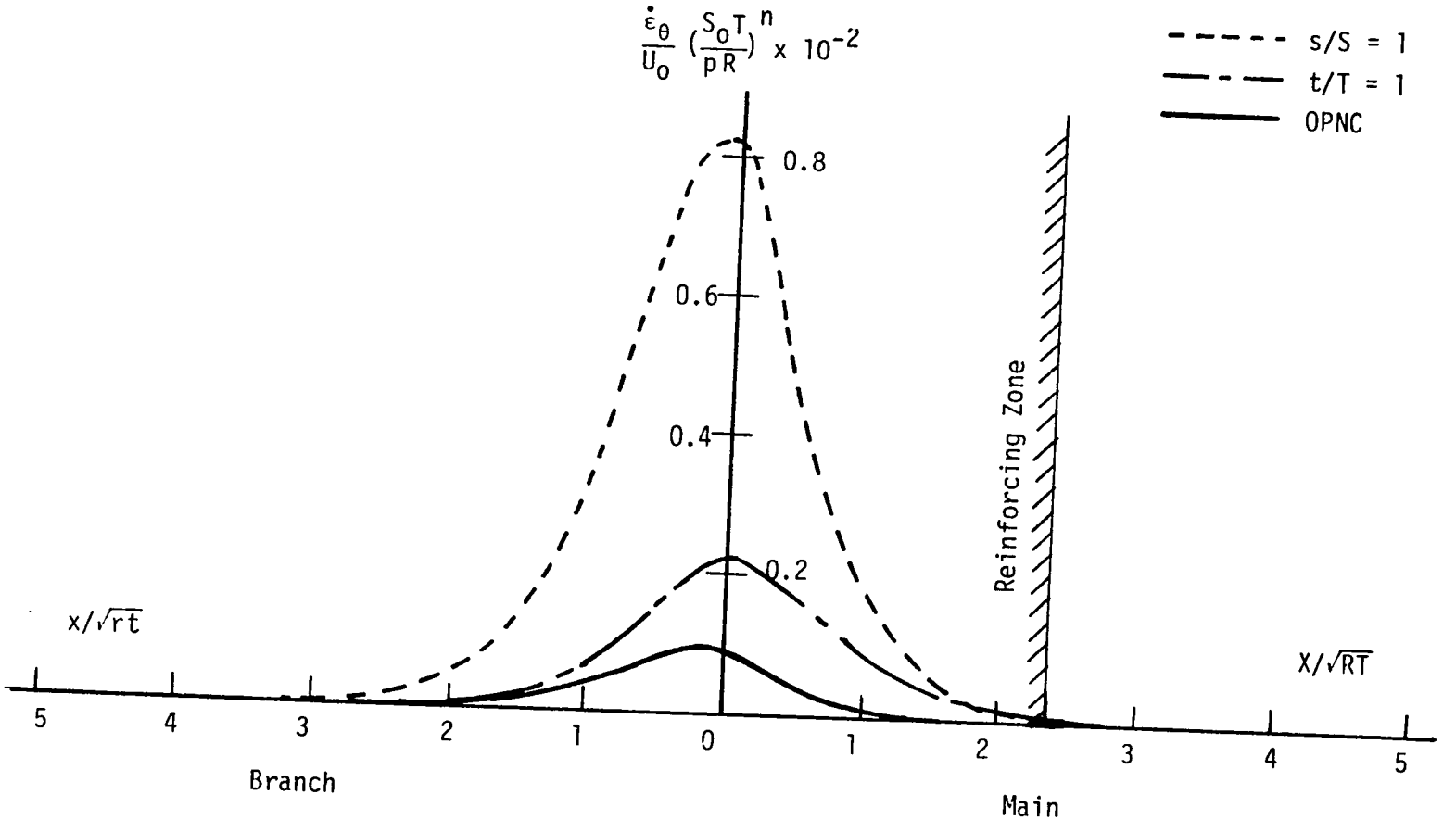

Fig. 13. Dimensionless Strain Rate in Circumferential Direction Along Pipe Axis

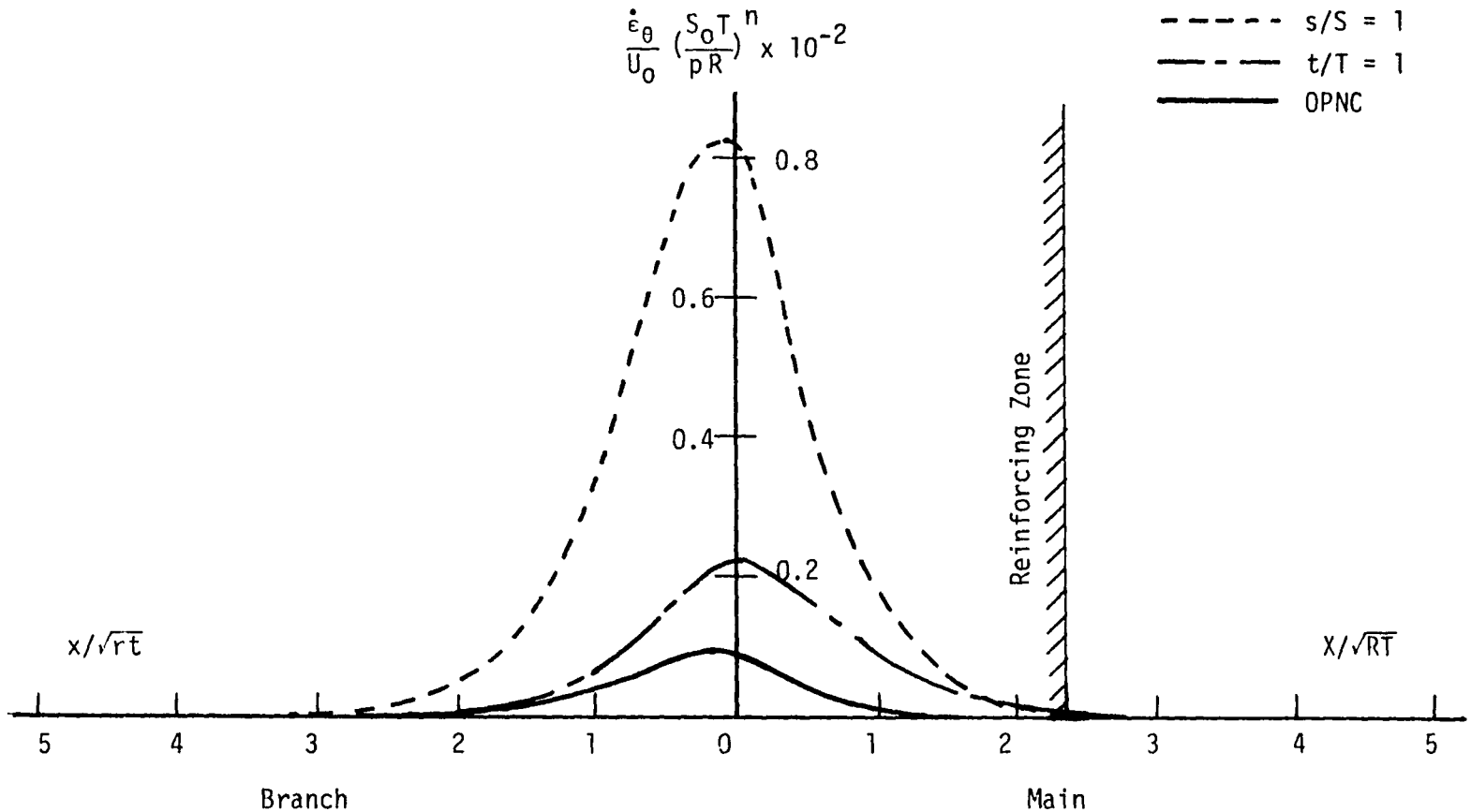

Fig. 13. Dimensionless Strain Rate in Circumferential Direction Along Pipe Axis

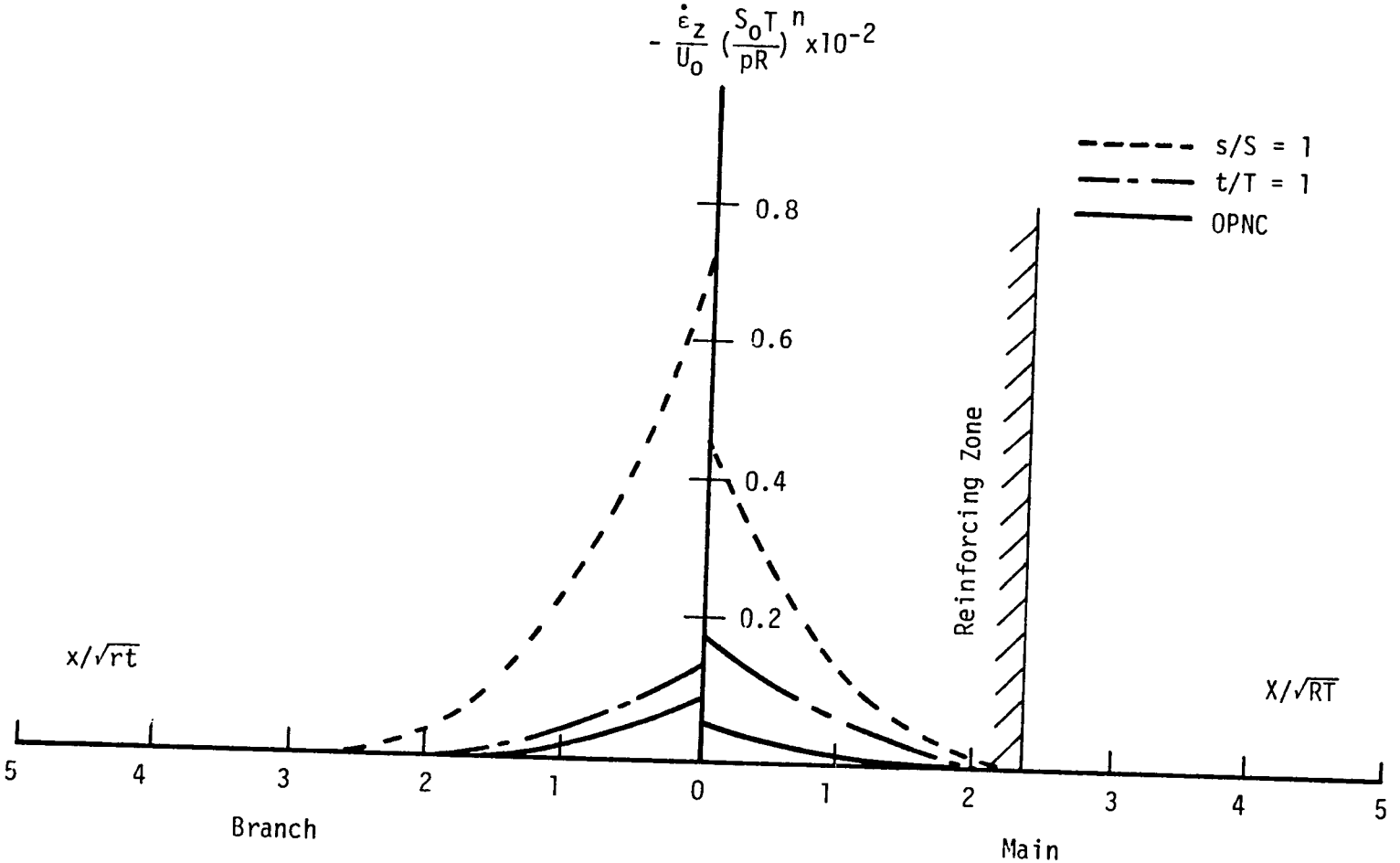

Fig. 14. Dimensionless Strain Rate in Thickness Direction Along Pipe Axis

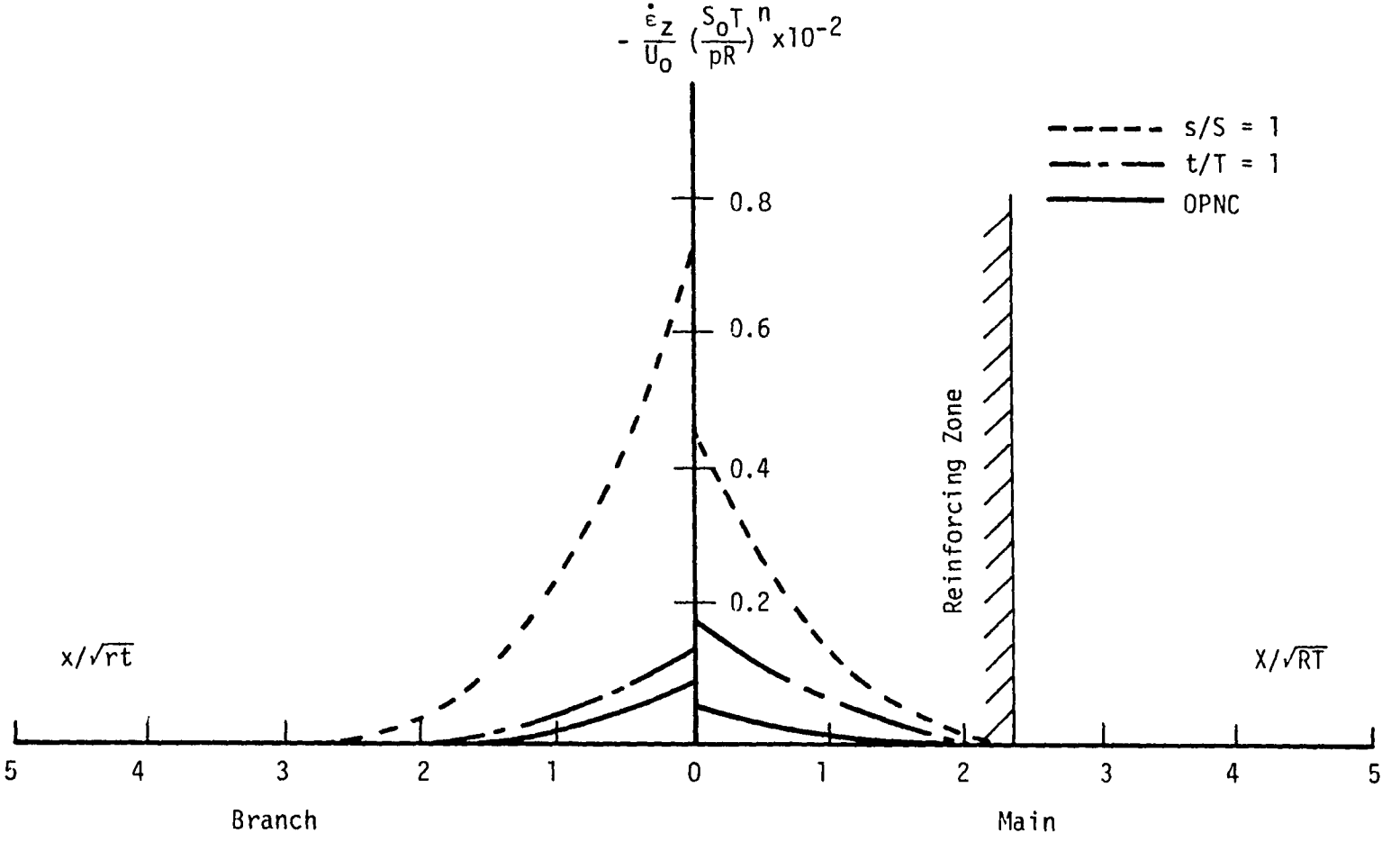

Fig. 14. Dimensionless Strain Rate in Thickness Direction Along Pipe Axis

Table 1. Dimensions and Material Properties

Case	r/R	R/T	r/t	s/S[1]	t/T	E	ν	n	U_o	S_o
s/s = 1	0.5	50	50	1	0.5	10^6	0.3	3	0.001	20
t/T = 1	0.5	50	25	0.5	1	10^6	0.3	3	0.001	20
OPNC	0.5	22.2[2]	50	1	0.5	10^6	0.3	3	0.001	20

Note:

(1) $s = \frac{pr}{t}$, $S = \frac{sR}{T}$ where p is internal pressure.

(2) This ratio is available within the reinforcing zone (see Appendix II) .

Table 1. Dimensions and Material Properties

Case	r/R	R/T	r/t	s/S[1]	t/T	E	ν	n	U_o	S_o
s/s = 1	0.5	50	50	1	0.5	10^6	0.3	3	0.001	20
t/T = 1	0.5	50	25	0.5	1	10^6	0.3	3	0.001	20
OPNC	0.5	22.2[2]	50	1	0.5	10^6	0.3	3	0.001	20

Note:

(1) $s = \frac{pr}{t}$, $S = \frac{sR}{T}$ where p is internal pressure.

(2) This ratio is available within the reinforcing zone (see Appendix II) .

Table 2. Nondimensional Stresses at Crotch Point
Elastic and Stationary Creep Solution

	Case	Main Pipe				Branch Pipe			
		$\sigma_x T/pR$		$\sigma_\theta T/pR$		$\sigma_x T/pR$		$\sigma_\theta T/pR$	
		Inside	Outside	Inside	Outside	Inside	Outside	Inside	Outside
Elastic	s/S = 1	-2.72	3.72	4.47	6.40	-12.38	13.38	1.57	9.30
	t/T = 1	-4.33	5.33	2.04	4.94	- 4.58	5.08	1.96	4.86
	OPNC	0.28	0.16	2.78	2.74	- 5.74	6.74	0.97	4.72
Stationary Creep	s/S = 1	-2.22	3.05	2.97	5.35	- 8.53	8.90	-2.81	5.80
	t/T = 1	-4.02	4.44	-0.48	3.55	- 4.11	4.31	-0.56	3.54
	OPNC	0.37	0.07	2.19	2.06	- 3.43	3.81	-0.85	2.63

Table 2. Nondimensional Stresses at Crotch Point
Elastic and Stationary Creep Solution

	Case	Main Pipe				Branch Pipe			
		$\sigma_x T/pR$		$\sigma_\theta T/pR$		$\sigma_x T/pR$		$\sigma_\theta T/pR$	
		Inside	Outside	Inside	Outside	Inside	Outside	Inside	Outside
Elastic	s/S = 1	-2.72	3.72	4.47	6.40	-12.38	13.38	1.57	9.30
	t/T = 1	-4.33	5.33	2.04	4.94	- 4.58	5.08	1.96	4.86
	OPNC	0.28	0.16	2.78	2.74	- 5.74	6.74	0.97	4.72
Stationary Creep	s/S = 1	-2.22	3.05	2.97	5.35	- 8.53	8.90	-2.81	5.80
	t/T = 1	-4.02	4.44	-0.48	3.55	- 4.11	4.31	-0.56	3.54
	OPNC	0.37	0.07	2.19	2.06	- 3.43	3.81	-0.85	2.63

Table 3. Dimensionless Average Equivalent Stress and Strain Rate at Crotch Point in Stationary State.

Case	$\sigma_e T/pR$		$\frac{\dot{\varepsilon}_\theta}{U_o}\left(\frac{S_o t}{pR}\right)^n$		$-\frac{\dot{\varepsilon}_z}{U_o}\left(\frac{S_o T}{pR}\right)^n$	
	Main	Branch	Main	Branch	Main	Branch
s/S = 1	4.58 (5.93)	7.68 (12.56)	82.5 (185)	82.6 (863)	49.2 (96)	70.8 (376)
t/T = 1	3.94 (5.39)	3.92 (5.40)	22.1 (97)	22.1 (100)	16.8 (50)	13.8 (39)
OPNC	2.03 (2.66)	3.24 (6.14)	8.3 (19)	8.3 (100)	4.8 (11)	8.2 (56)

Note: Elastically calculated values are shown in ( ).

Table 3. Dimensionless Average Equivalent Stress and Strain Rate at Crotch Point in Stationary State.

Case	$\sigma_e T/pR$		$\frac{\dot{\varepsilon}_\theta}{U_o}\left(\frac{S_o t}{pR}\right)^n$		$-\frac{\dot{\varepsilon}_z}{U_o}\left(\frac{S_o T}{pR}\right)^n$	
	Main	Branch	Main	Branch	Main	Branch
s/S = 1	4.58 (5.93)	7.68 (12.56)	82.5 (185)	82.6 (863)	49.2 (96)	70.8 (376)
t/T = 1	3.94 (5.39)	3.92 (5.40)	22.1 (97)	22.1 (100)	16.8 (50)	13.8 (39)
OPNC	2.03 (2.66)	3.24 (6.14)	8.3 (19)	8.3 (100)	4.8 (11)	8.2 (56)

Note: Elastically calculated values are shown in ( ).

REFERENCES

1. Updike, D.P., and Kalnins, A. "Creep of Intersecting Equal Diameter Cylindrical Shells under Internal Pressure", ASME paper 82-PVP-55 (1982).

2. Updike, D.P., "Approximate Elastic Stresses in a Tee Branch Pipe Connection Under Internal Pressure", Trans. of the ASME, Jr. of Pressure Vessel Technology, Vol. 103 (1981), pp. 103-107.

3. Updike, D.P., and Kalnins, A. "Approximate Analysis of Intersecting Equal Diameter Cylindrical Shells Under Internal Pressure", ASME paper 79-PVP-2 (1979).

4. Kalnins, A., "Analysis of Shells of Revolution Subjected to Symmetric and Nonsymmetric Loads", Trans. of the ASME, Jr. of Applied Mechanics, Vol. 31 (1964), pp. 467-476.

5. Kalnins, A., and Lestingi, J.F., "On Nonlinear Analysis of Elastic Shells of Revolution", Trans. of the ASME, Jr. of Applied Mechanics, Vol. 34 (1967), pp. 59-64.

6. Hult, J., Creep in Engineering Structures, Blaisdell Publ Co., Waltham, MA, U.S.A.

7. Finnie, I., and Heller, W.R., Creep in Engineering Materials, McGraw-Hill Book Co., New York, 1959.

8. Penny, R.K., and Marriott, D.L., Design for Creep, McGraw Hill Co., London, 1974.

9. Kalnins, A., Updike, D.P., and Yang, S.J., "Creep Analysis of Shells", preprint of 6th SMIRT at Paris, L11-4, (1981).

10. The ASME, ASME Boiler and Pressure Vessel Code: Section III Nuclear Power Plant Components Div. 1, Subsection NC, Class 2 components, (1980).

Appendix I

The following problems are calculated for the purpose of checking the transfer matrix of Eq. (11) in chapter II.

Problem No. 1: Elastic, equal diameter and thickness, compared with the results of [1].

Problem No. 2: Elastic, different diameter and thickness, compared with the results of [2].

Problem No. 3: Creep, same as No. 1

Problem No. 4: Creep, two cases which is mirror image to the other respectively, checked the difference of the results of integration direction.

From the next page, the model of each problem is shown including dimensions, material properties, calculation model and the results with the reference data.

Problem No. 1 [Elastic]

r/R = 1, R/T = r/t = 100, t/T = 1, s/S = 1

$E = 10^6$, $\nu = 0.3$

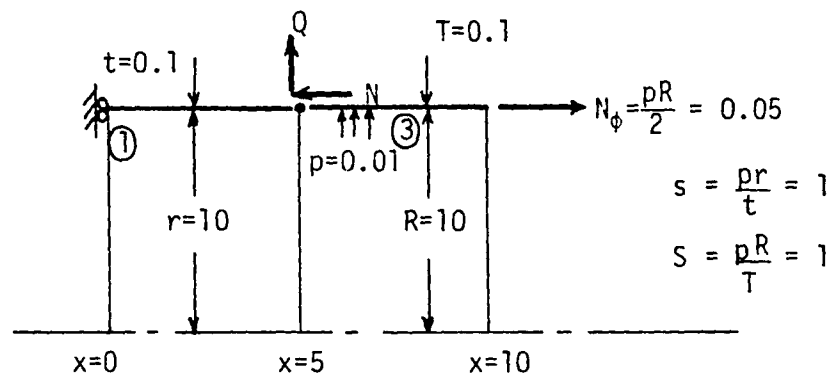

$Q = p\,R = 0.1$ $\qquad N = (\frac{R^2 - r^2}{2R})p = 0$

Results

End of part ①

	$\sigma_x T/pR$		$\sigma_\theta T/pR$	
	in	out	in	out
	-11.17	12.17	3.926	10.93
[1]	-11.17	12.17	3.93	10.93

Start of part ③

	$\sigma_x T/pR$		$\sigma_\theta T/pR$	
	in	out	in	out
	-11.17	12.17	3.926	10.93
[1]	-11.17	12.17	3.93	10.93

Problem No. 2 [Elastic]

r/R = 0.5, R/T = 50, r/t = 50, t/T = 0.5, s/S = 1

E = 1.0 , b = 0.3

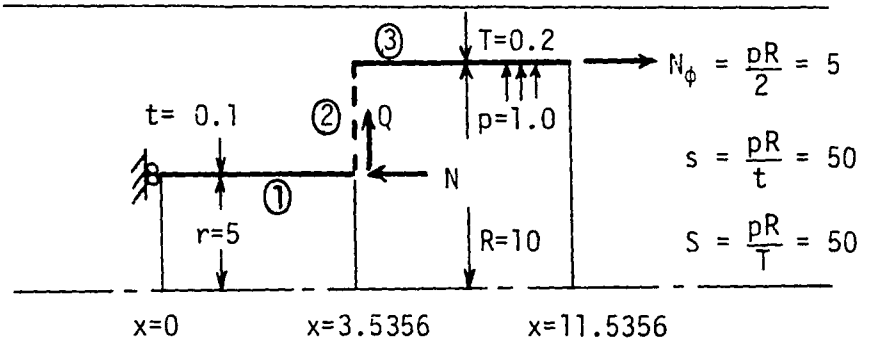

$Q = pR = 10$, $N = -(\frac{R^2-r^2}{2r})p = -7.5$

Results

End of part ① (Branch)

	$\sigma_X T/pR$		$\sigma_\theta T/pR$	
	in	out	in	out
	-619.0	669.0	78.47	464.9
			271.685 (average)	
[2]	-618.8	668.8	271.7	

Start of part ③ (Main)

	$\sigma_X T/pR$		$\sigma_\theta T/pR$	
	in	out	in	out
	-136.0	186.0	223.4	320
			271.7 (average)	
[2]	-135.95	185.95	271.7	

Problem No. 3 [Creep]

$r/R = 1$, $R/T = r/t = 100$, $t/T = 1$, $s/S = 1$

$E = 10^6$, $\nu = 0.3$, $n = 5$, $U_o = 0.001$, $S_o = 1$

Same as Problem No. 1

Results: Stationary creep solution

	$\sigma_x T/pR$		$\sigma_\theta T/pR$	
	in	out	in	out
	-8.615	8.876	-2.259	6.303
[1]	-8.53	8.80	-2.03	6.46

Note: End of part ① and start of part ③ are completely the same.

In Fig. A1, the relationship between a dimensionless equivalent stress of crotch point versus a dimensionless time parameter is shown.

Problem No. 4 [Creep]

$r/R = 0.5$, $R/T = r/t = 50$, $t/T = 1$, $s/S = 0.5$

$E = 10^6$, $\nu = 0.3$, $n = 3$, $U_0 = 0.001$, $S_0 = 20$

Case A

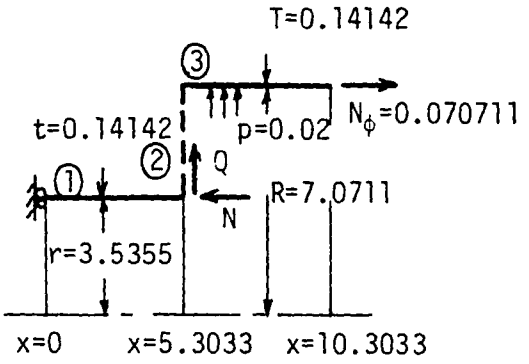

$Q = pR = 0.1414$

$N = -(\frac{R^2-r^2}{2r})p = -0.1061$

Case B

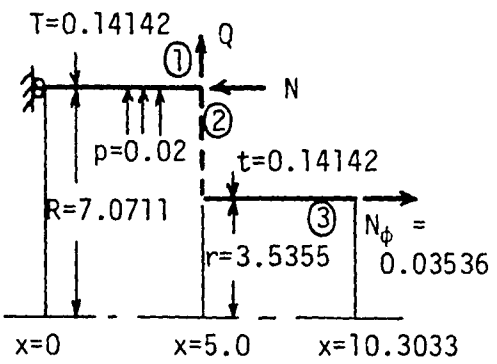

$Q = pr = 0.070711$

$N = -(\frac{R^2-r^2}{2R})p = -0.05303$

Results

In Table A1, the relationship between a dimensionless equivalent stress of crotch point versus a dimensionless time parameter is shown. It is clear from Table A1 that the two cases result in the mirror image of the other respectively.

Therefore, negligible differences occur depending on the integration direction.

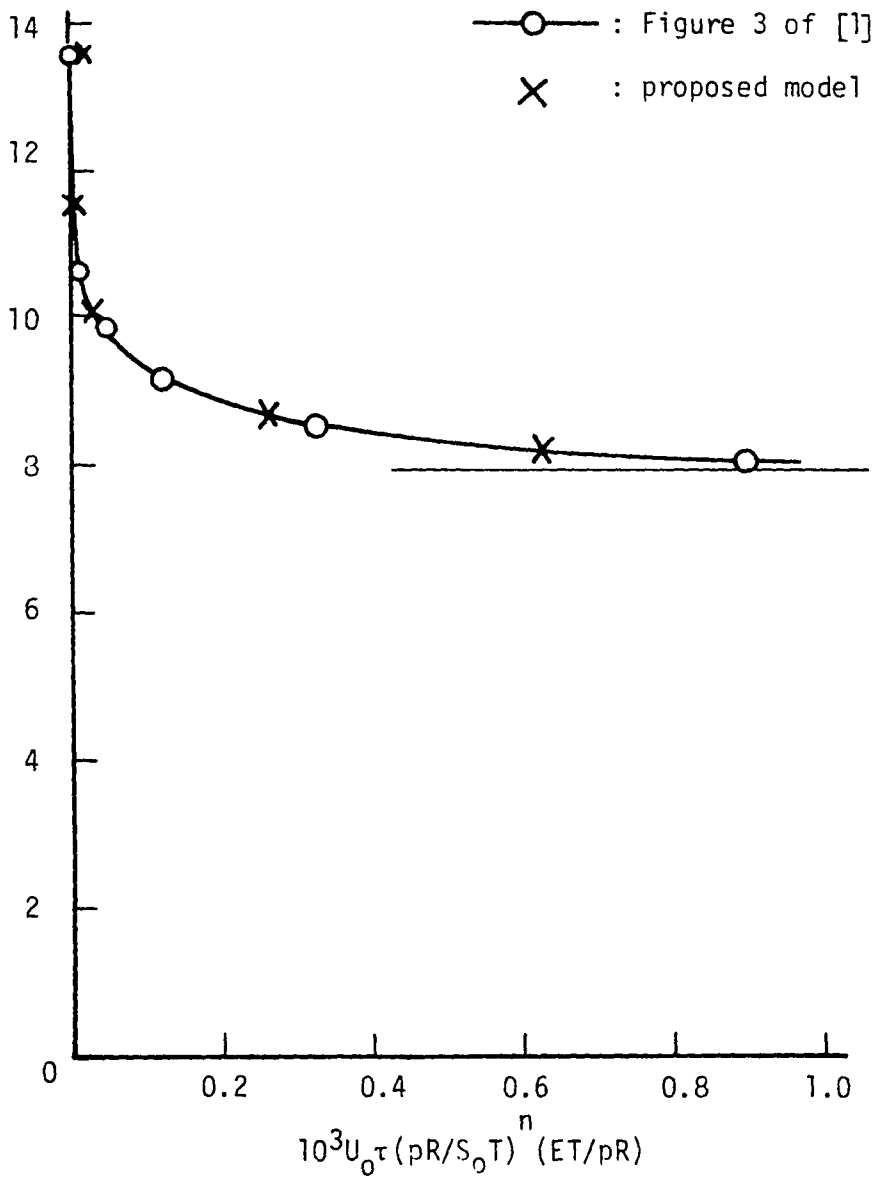

Fig. A1. Dimensionless Equivalent Stress at Inside of Crotch Point Versus A Dimensionless Time Parameter

Table A1. Dimensionless Equivalent Stress Versus Dimensionless Time Parameter

Time Step	α (1)	$\sigma_e T/pR$	
		Case A (2)	Case B (2)
1	0.0	5.817 (① - 5.303)	5.818 (③ - 0.0)
2	0.009	5.073 (① - 5.303)	5.073 (③ - 0.0)
3	0.033	4.614 (③ - 0.0)	4.615 (① - 5.0)
4	0.092	4.280 (③ - 0.0)	4.280 (① - 5.0)
5	0.239	4.116 (③ - 0.0)	4.116 (① - 5.0)
6	0.608	4.081 (③ - 0.0)	4.082 (① - 5.0)
7	1.529	4.068 (③ - 0.0)	4.069 (① - 5.0)
8	3.831	4.074 (③ - 0.0)	4.075 (① - 5.0)

Note:

(1) $\alpha = U_{0\tau} t(pR/S_0T)^n(ET/pR)$

(2) Location of the maximum $\sigma_e T/pR$ is shown in ( ).
ex: (① - 5.303) means at x=5.303 of part ① .

Appendix II

The opening compensation method of pressure vessels or pipes is given in a design code such as ASME Boiler and Pressure Vessel Code [10].

A reinforcement design according to NC-3643.3 of [10] is shown in Fig. A2. In designing the reinforcement it is assumed here that the required thickness of the main and the branch (T_{mh} and T_{mb}) are the same as the nominal thickness of the both pipes (T_h and T_b).

In the following, the reinforcement design calculation is shown.

Required Area $A_o = 1.07\ (T_{mh})(d_1)$

$= 1.07 \times 0.14142 \times 7.0 = 1.06$

$A_1 = d_2(T_h - T_{mh}) = 7.0 \times (0.14142 - 0.14142) = 0$

$d_2 = \text{Min}[D_{ob}, \text{Max}\ (d_1, T_b + T_h + d_1/2)]$

$= \text{Min}\ [7.1417, \text{Max}\ (7.0, 3.677)]$

$= 7.0$

$A_2 = 2L(T_b - T_{mb}) = 2 \times 1.768 \times (0.070711 - 0.070711) = 0$

$L = 2.5\ T_b = 2.5 \times 0.070711 = 0.1768$

$A_3 = L(2d_2 - D_{ob}) = 0.1768 \times (2 \times 7.0 - 7.1417)$

$= 1.213$

Therefore,

$$A_1 + A_2 + A_3 = 1.175 > A_0 = 1.048$$

The dimensions of reinforced tee branch connection are shown in Fig. A3.

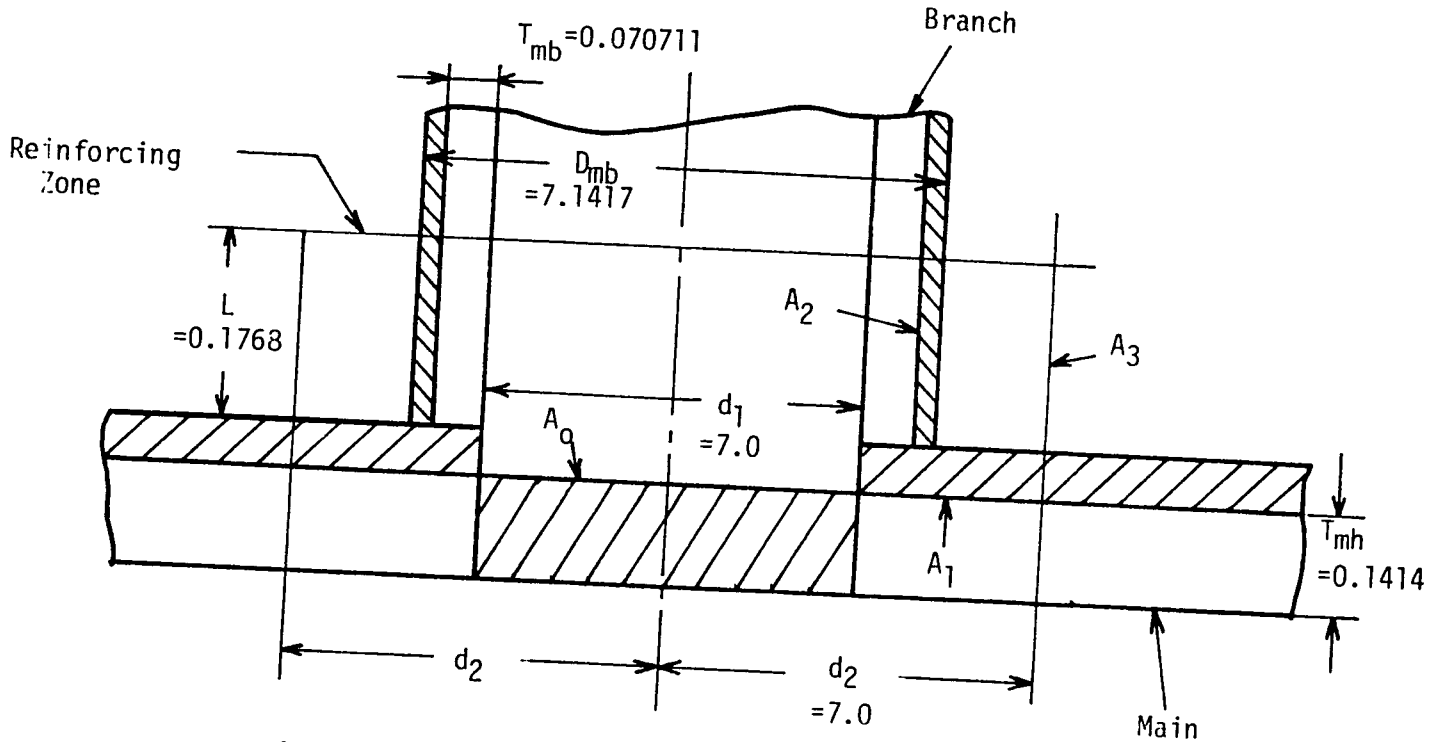

Area A_1 - Excess Wall in Main
Area A_2 - Excess Wall in Branch

Fig. A2. Reinforcement of Branch Connection

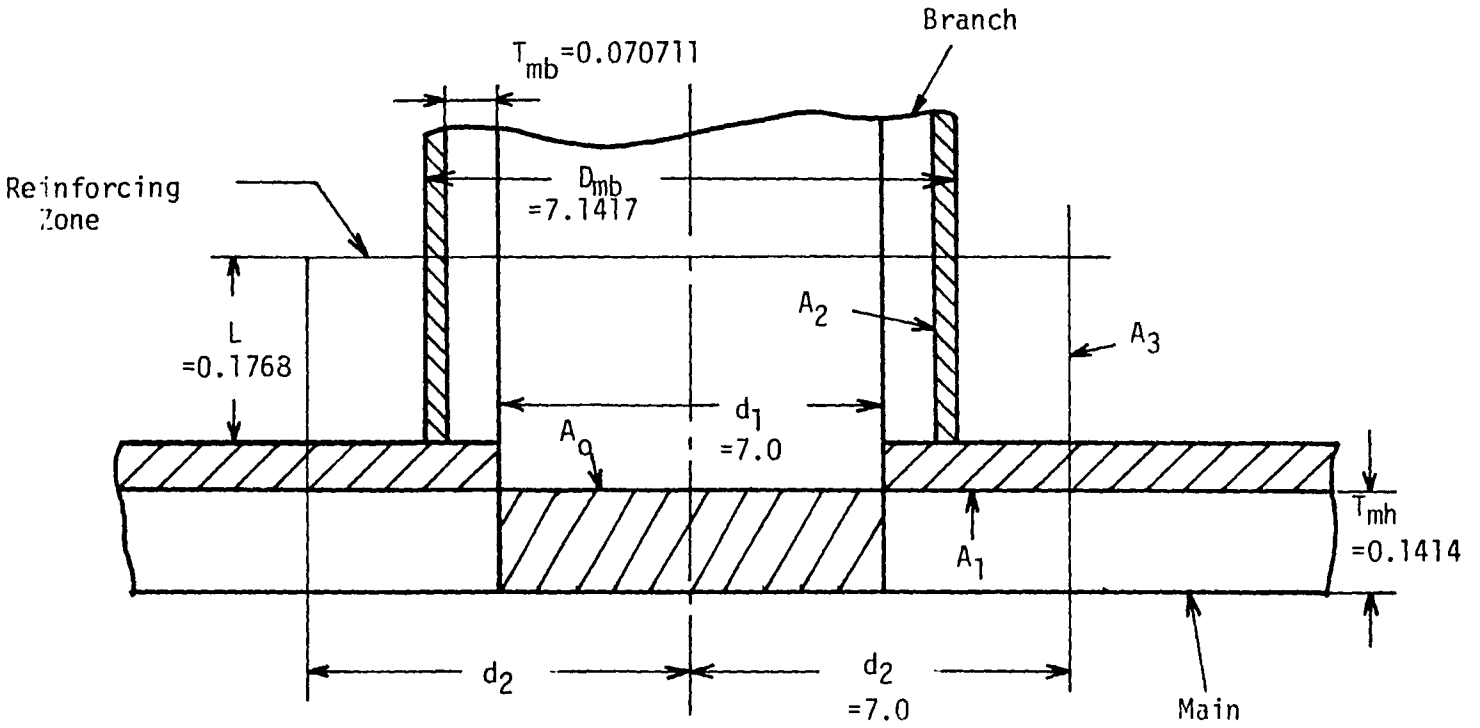

Area A_1 - Excess Wall in Main
Area A_2 - Excess Wall in Branch

Fig. A2. Reinforcement of Branch Connection

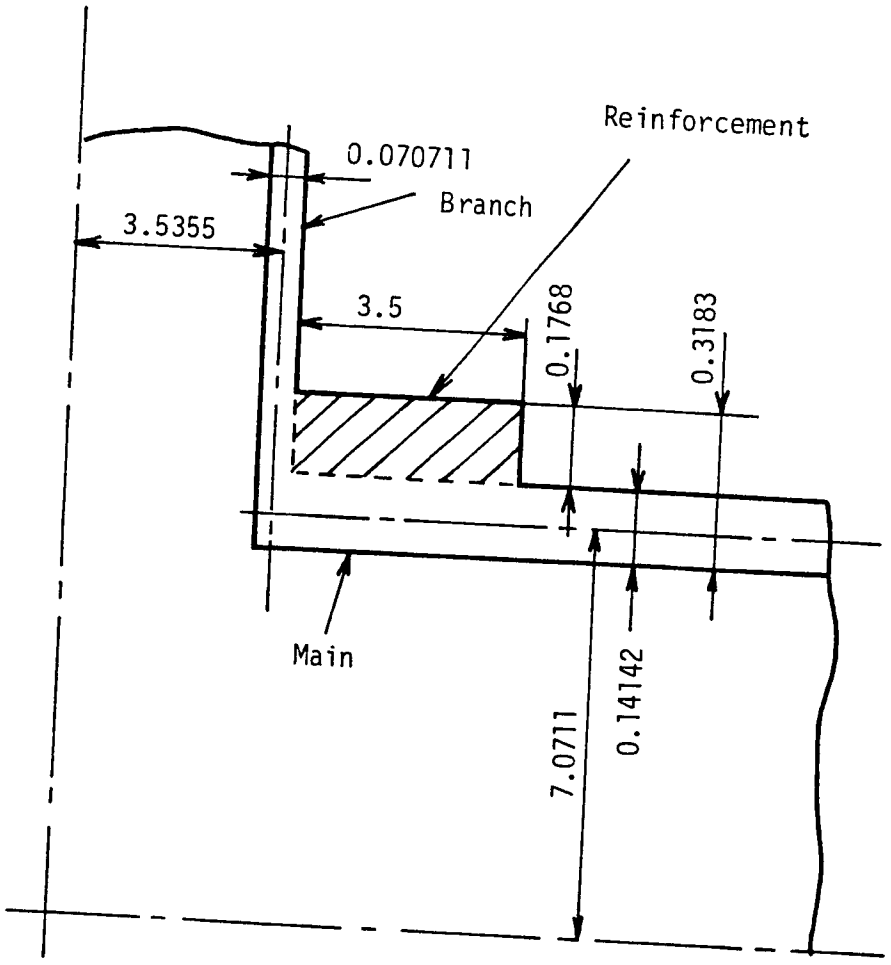

Fig. A3. Reinforced Equal Strength Tee Branch Connection

VITA

Takenori Shindo was born in Kagawa-Ken, Japan on September 30, 1946 to Mrs. Shizue Shindo and Mr. Masao Shindo. He graduated from National Okayama University in March 1969 with a B.S. degree in the Department of Mechanical Engineering, School of Engineering.

In April 1969, the author entered Babcock-Hitachi K.K. in Tokyo, Japan as a design engineer.

He has been working as a stress analyst for twelve years before coming to Lehigh University in August 1981. His company gave him a chance to go abroad to study for one year in 1981. He studied mainly solid mechanics in Lehigh University.